

**Physisorption-Induced Structural Change Directing Carbon Monoxide Chemisorption
and Nitric Oxide Coordination on Hemilabile Porous Metal Organic Framework
 $\text{NaNi}_3(\text{OH})(\text{SIP})_2(\text{H}_2\text{O})_5 \cdot \text{H}_2\text{O}$ (SIP = 5-sulfoisophthalate)**

Jon.G. Bell¹, Samuel. A. Morris², Farida. Aidoudi², Laura J. McCormick^{2,3}, Russell E. Morris², K. Mark Thomas^{1*}

¹Wolfson Northern Carbon Reduction Laboratories, School of Chemical Engineering and Advanced Materials, Newcastle University, Newcastle upon Tyne, NE1 7RU, U.K.

*Email: mark.thomas@ncl.ac.uk

²School of Chemistry, Purdie Building, St Andrews University, North Haugh, St Andrews, Fife KY16 9ST, U.K.

³Experimental Systems Group, Advanced Light Source, Berkeley, California, USA

Supporting Information

| Contents | Page |
|--|-------------|
| S1 Activation of porous structure | S4 |
| S1.1 Temperature Programmed Thermogravimetric analysis of NaCo ₃ (OH)(SIP) ₂ (H ₂ O) ₅ ·H ₂ O and NaNi ₃ (OH)(SIP) ₂ (H ₂ O) ₅ ·H ₂ O under ultra-high vacuum using the IGA system | S4 |
| S1.2 Powder X-ray diffraction profiles and crystallographic information | S4 |
| S2 CO adsorption/desorption isotherms | S8 |
| S2.1 NaNi ₃ (OH)(SIP) ₂ | S8 |
| S2.1.1 CO adsorption isotherms for NaNi ₃ (OH)(SIP) ₂ | S8 |
| S2.1.2 CO low pressure kinetic desorption profile | S11 |
| S2.1.3 CO loading experiments | S12 |
| S2.1.4 Activation of NaNi ₃ (OH)(SIP) ₂ (H ₂ O) ₅ ·H ₂ O under ultra-high vacuum at 403 K to give NaNi ₃ (OH)(SIP) ₂ (H ₂ O) ₂ for comparison with XRD measurements | S14 |
| S2.1.5 CO desorption kinetics for NaNi ₃ (OH)(SIP) ₂ (H ₂ O) ₂ degassed at 403 K | S15 |
| S2.2 NaCo ₃ (OH)(SIP) ₂ | S15 |
| S2.2.1 CO adsorption/desorption isotherms for NaCo ₃ (OH)(SIP) ₂ after degas at 448 K | S15 |
| S2.2.2 CO desorption kinetic profile for NaCo ₃ (OH)(SIP) ₂ degassed at 448 K | S16 |
| S3 Comparison of carbon dioxide adsorption before and after CO adsorption | S17 |
| S4 Virial analysis | S18 |
| S4.1 CO adsorption on NaNi ₃ (OH)(SIP) ₂ | S18 |
| S4.2 CO adsorption on NaCo ₃ (OH)(SIP) ₂ | S20 |
| S5 Clausius-Clapeyron Graphs | S21 |
| S5.1 CO adsorption on NaNi ₃ (OH) ₂ (SIP) ₂ | S21 |
| S5.2 CO adsorption on NaCo ₃ (OH) ₂ (SIP) ₂ (degas temperature 448 K) | S22 |
| S6 Enthalpy and entropy of adsorption for NaNi₃(OH)(SIP)₂ and NaCo₃(OH)(SIP)₂ | S23 |
| S7 Ideal adsorbed solution theory: CO/ N₂ selectivity at 348 K | S29 |

| | | |
|-------------|---|-----|
| S7.1 | Comparison of CO and N ₂ adsorption isotherms for NaNi ₃ (OH)(SIP) ₂ and NaCo ₃ (OH)(SIP) ₂ at 348 K | S30 |
| S7.2 | Comparison of CO/N ₂ selectivity for adsorption of 1:1 mixture on NaNi ₃ (OH)(SIP) ₂ and NaCo ₃ (OH)(SIP) ₂ at 348 K | S32 |
| S8 | In-situ temperature programmed desorption (TPD) studies | S33 |
| S8.1 | NaNi₃(OH)(SIP)₂ | S33 |
| S8.1.1 | In-situ TPD under ultra-high vacuum after sequential CO isotherms | S33 |
| S8.1.2 | In-situ temperature programmed desorption with simultaneous thermogravimetric and dynamic mass spectrometry under helium for NaNi ₃ (OH)(SIP) ₂ after CO treatment for 2 weeks at 348 K | S34 |
| S9 | Temperature programmed thermogravimetric analysis coupled with mass spectrometry in flowing helium (ex-situ measurements) | S36 |
| S9.1 | Experimental | S36 |
| S9.2 | Results and Discussion | S36 |
| S10 | Scanning electron microscopy | S41 |
| | References | S42 |

S1 Activation of porous structure

S1.1 Thermogravimetric analysis $\text{NaCo}_3(\text{OH})(\text{SIP})_2(\text{H}_2\text{O})_5 \cdot \text{H}_2\text{O}$ and $\text{NaNi}_3(\text{OH})(\text{SIP})_2(\text{H}_2\text{O})_5 \cdot \text{H}_2\text{O}$ of under ultra-high vacuum using the IGA system

The Temperature Programmed Thermogravimetric Profiles give the following stoichiometry:
degas 400 K - $\text{NaNi}_3(\text{OH})(\text{SIP})_2(\text{H}_2\text{O})_2$ and degas at > 500 K - $\text{NaNi}_3(\text{OH})(\text{SIP})_2$

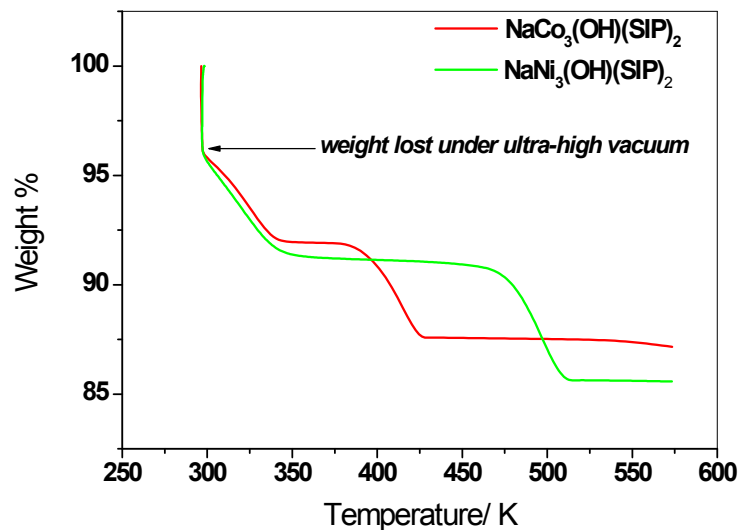
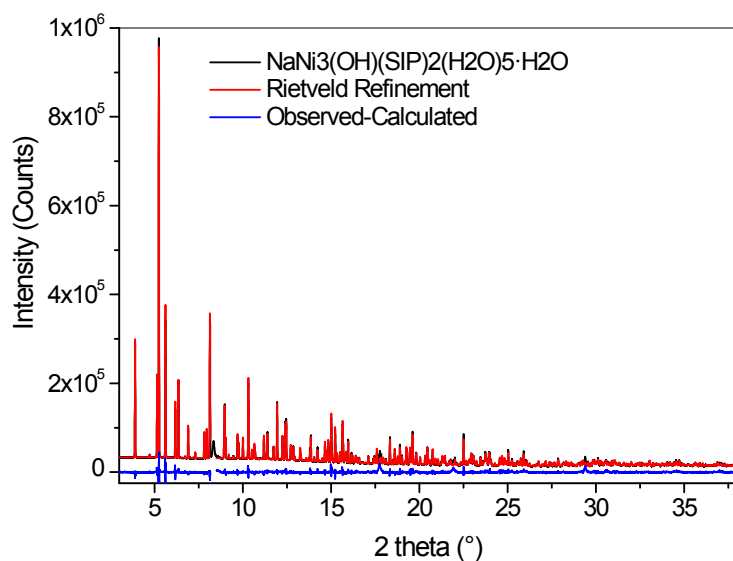


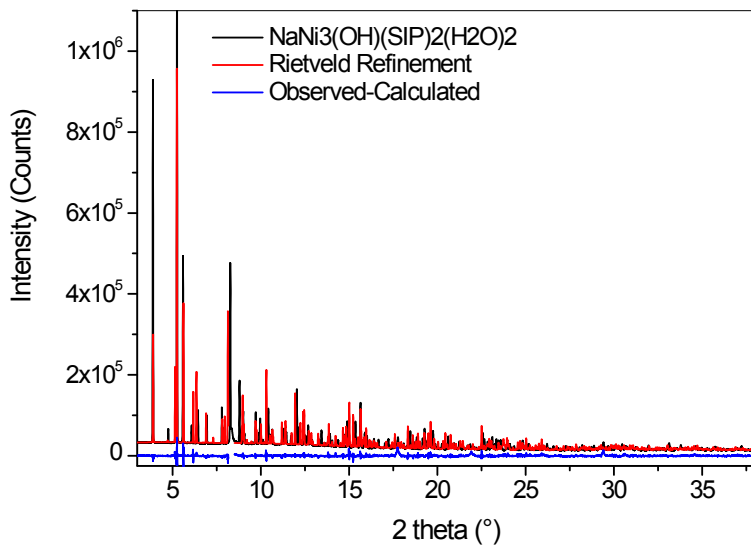
Figure S1. Temperature programmed thermogravimetric profiles for $\text{NaCo}_3(\text{OH})(\text{SIP})_2(\text{H}_2\text{O})_5 \cdot \text{H}_2\text{O}$ and $\text{NaNi}_3(\text{OH})(\text{SIP})_2(\text{H}_2\text{O})_5 \cdot \text{H}_2\text{O}$ under ultra-high vacuum at a heating rate of 1 K min^{-1}

S1.2 Powder X-ray diffraction profiles and crystallographic information

a)



b)



c)

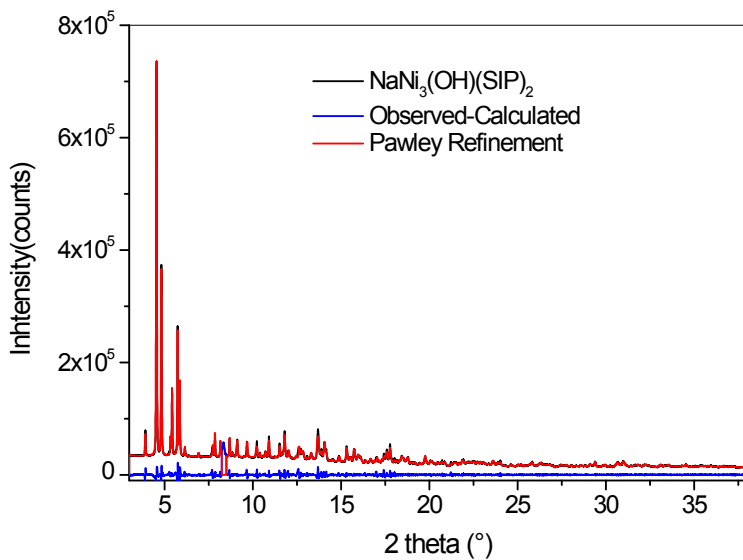


Figure S2 PXRD profiles for a) $\text{NaNi}_3(\text{OH})(\text{SIP})_2(\text{H}_2\text{O})_5 \cdot \text{H}_2\text{O}$ (Rietveld Refinement from $3 - 38^\circ$ gave $R_{wp} = 6.84\%$ in the space group P-1. Black line is the experimental data, red is the calculated fit and the blue is the difference curve); b) $\text{NaNi}_3(\text{OH})(\text{SIP})_2(\text{H}_2\text{O})_2$ degassed under vacuum at 400 K (Rietveld Refinement from $3 - 38^\circ$). gave $R_{wp} = 7.14\%$ in the space group P-1. Black line is the experimental data, red is the calculated fit and the blue is the difference curve; c) $\text{NaNi}_3(\text{OH})(\text{SIP})_2$ degassed at 573 K (Pawley refinement gave $R_{wp} = 4.68\%$ in space group P-1. Black line is the experimental data, red is the calculated fit and the blue is the difference curve)

Fresh $\text{NaNi}_3(\text{OH})(\text{SIP})_2(\text{H}_2\text{O})_5 \cdot \text{H}_2\text{O}$. CIF file RT-1
Space Group P-1. $a = 9.8590(11) \text{ \AA}$, $b = 11.0355(13) \text{ \AA}$, $c = 12.567(14) \text{ \AA}$, $\alpha = 104.782(2)^\circ$, $\beta = 89.974(2)^\circ$, $\gamma = 109.954(2)^\circ$, $V = 1237.01 \text{ \AA}^3$

Degas 400 K $\text{NaNi}_3(\text{OH})(\text{SIP})_2(\text{H}_2\text{O})_2$. CIF file 400K-1 and 400K-2
Cif file 400K-1: Space Group P-1. $a = 9.8415(13) \text{ \AA}$, $b = 11.0066(15) \text{ \AA}$, $c = 12.6355(17) \text{ \AA}$, $\alpha = 104.131(3)^\circ$, $\beta = 92.127(3)^\circ$, $\gamma = 110.798(3)^\circ$, $V = 1229.17 \text{ \AA}^3$

NO Reaction with $\text{NaNi}_3(\text{OH})(\text{SIP})_2(\text{H}_2\text{O})_2$. CIF File 400K-NO

Space Group P-1. $a = 9.8979(17) \text{ \AA}$, $b = 10.9915(18) \text{ \AA}$, $c = 12.589(2) \text{ \AA}$, $\alpha = 104.603(3)^\circ$, $\beta = 91.331(3)^\circ$, $\gamma = 110.658(3)^\circ$, $V = 1230.58 \text{ \AA}^3$

CO Reaction with $\text{NaNi}_3(\text{OH})(\text{SIP})_2(\text{H}_2\text{O})_2$. CIF File 400K-CO

Space Group P-1. $a = 9.8418(16) \text{ \AA}$, $b = 10.9891(18) \text{ \AA}$, $c = 12.587(2) \text{ \AA}$, $\alpha = 104.340(3)^\circ$, $\beta = 91.715(3)^\circ$, $\gamma = 110.678(3)^\circ$, $V = 1223.55 \text{ \AA}^3$

Degas 448 K $\text{NaCo}_3(\text{OH})(\text{SIP})_2$: CIF file NaCoSIP

Space Group P-1. $a = 9.972(4) \text{ \AA}$, $b = 11.192(5)(15) \text{ \AA}$, $c = 12.679(5) \text{ \AA}$, $\alpha = 104.544(9)^\circ$, $\beta = 90.078(9)^\circ$, $\gamma = 110.086(9)^\circ$, $V = 1280.42 \text{ \AA}^3$

Degas 573 K PXRD $\text{NaNi}_3(\text{OH})(\text{SIP})_2$

Space Group P-1 with unit cell dimensions and this gave the following: $a = 10.8516(5) \text{ \AA}$, $b = 11.1792(5) \text{ \AA}$, $c = 12.5215(5) \text{ \AA}$, $\alpha = 98.575(3)^\circ$, $\beta = 106.154(3)^\circ$, $\gamma = 67.916(3)^\circ$, $V = 1350.3(1) \text{ \AA}^3$

CCDC Numbers for CIP Files

CoNaSIP = CCDC 1553467

RT-1 = CCDC 1553050

400K-1 = CCDC 1553052

400K-CO = CCDC 1553053

400K-NO = CCDC 1553051

Calculation of void volume of fully dehydrated $\text{NaNi}_3(\text{OH})(\text{SIP})_2$

Void volume for $\text{NaNi}_3(\text{OH})(\text{SIP})_2(\text{H}_2\text{O})_5 \cdot \text{H}_2\text{O} = 25 \text{ \AA}^3 / 1237.0 \text{ \AA}^3$

Void volume for $\text{NaNi}_3(\text{OH})(\text{SIP})_2(\text{H}_2\text{O})_2 = 190.1 \text{ \AA}^3 / 1229.2 \text{ \AA}^3$

Framework volume for $\text{NaNi}_3(\text{OH})(\text{SIP})_2(\text{H}_2\text{O})_2 = 1039.1 \text{ \AA}^3$

$\text{NaNi}_3(\text{OH})(\text{SIP})_2(\text{H}_2\text{O})_5 \cdot \text{H}_2\text{O}$ has 5 framework bound water molecules. Removal of 3 removed by partial dehydration to give $\text{NaNi}_3(\text{OH})(\text{SIP})_2(\text{H}_2\text{O})_2$, resulted in an increase in pore volume of $190.1 - 25 \text{ \AA}^3 = 165.1 \text{ \AA}^3$, i.e. approximately 55 \AA^3 per water.

The loss of a further two water molecules from $\text{NaNi}_3(\text{OH})(\text{SIP})_2(\text{H}_2\text{O})_2$ to give $\text{NaNi}_3(\text{OH})(\text{SIP})_2$, leads to a fully dehydrated framework volume of $1039.1 \text{ \AA}^3 - (2 * 55 \text{ \AA}^3) = 929.1 \text{ \AA}^3$.

Cell volume for $\text{NaNi}_3(\text{OH})(\text{SIP})_2$ from Pawley fit = 1350.3 \AA^3

Void volume for $\text{NaNi}_3(\text{OH})(\text{SIP})_2 = 1350.3 \text{ \AA}^3 - 929.1 \text{ \AA}^3 = 421.2 \text{ \AA}^3$

Void volume (%) for $\text{NaNi}_3(\text{OH})(\text{SIP})_2 = 421.2 \text{ \AA}^3 / 1350.3 \text{ \AA}^3 = 31.2\%$

Density of $\text{NaNi}_3(\text{OH})(\text{SIP})_2$ framework = 1.728 g cm^{-3}

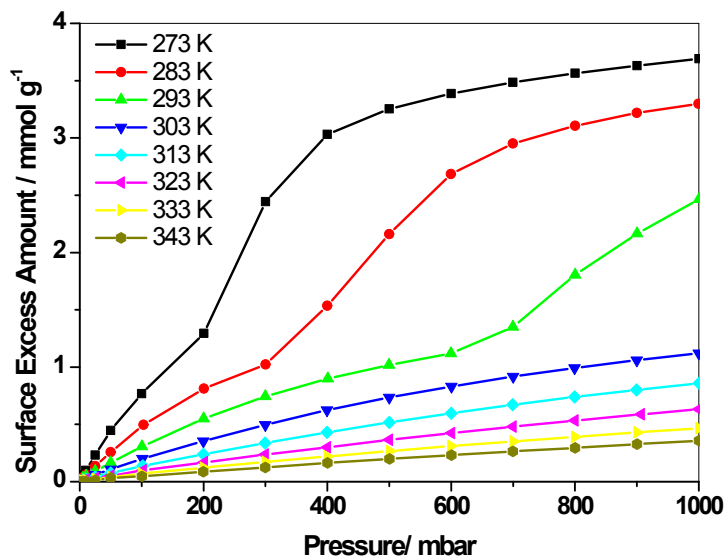
Crystallographic void volume = $0.1805 \text{ cm}^3 \text{ g}^{-1}$

S2 CO adsorption isotherms

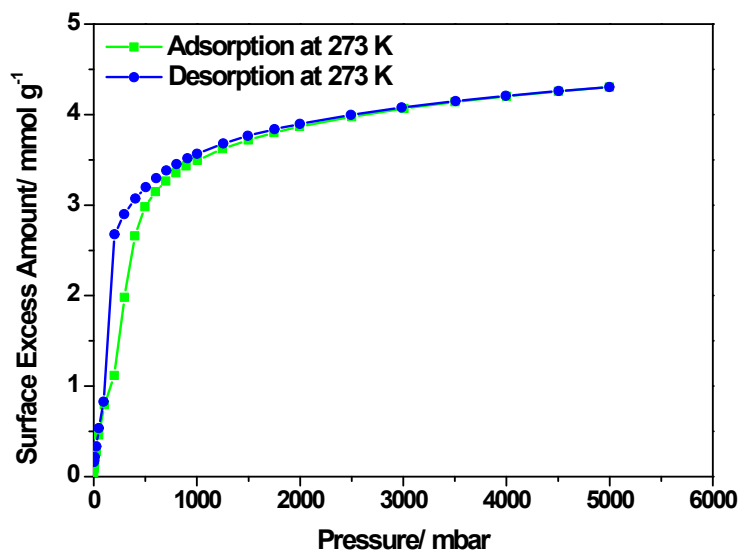
S2.1 NaNi₃(OH)(SIP)₂

S2.1.1 CO adsorption/desorption isotherms for NaNi₃(OH)(SIP)₂

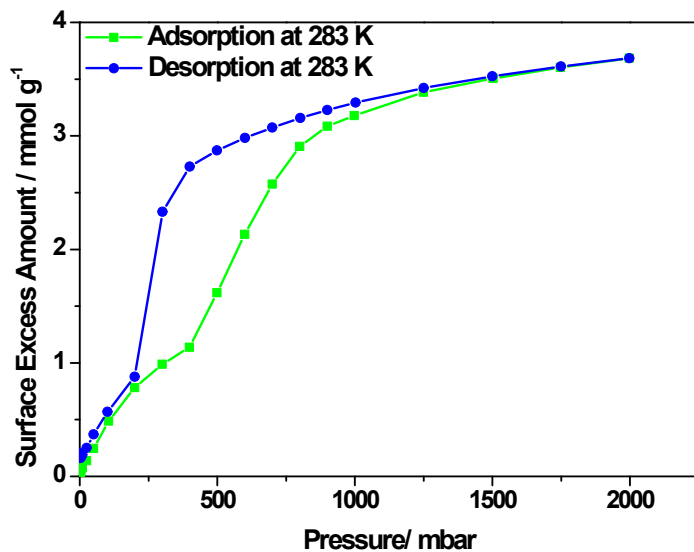
a)



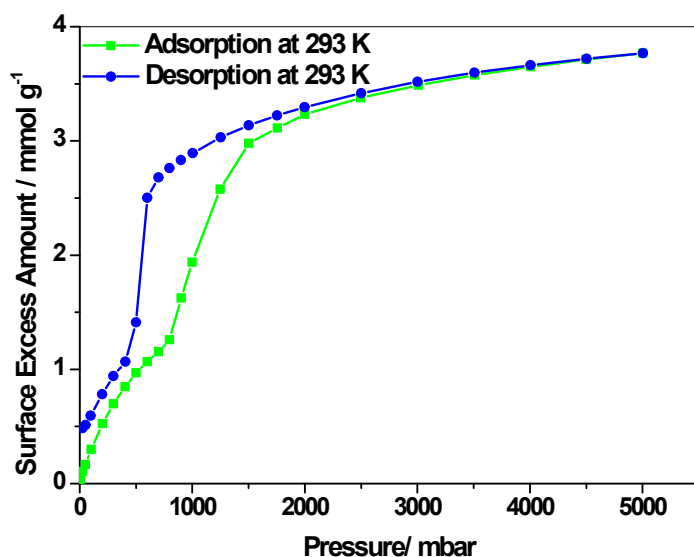
b)



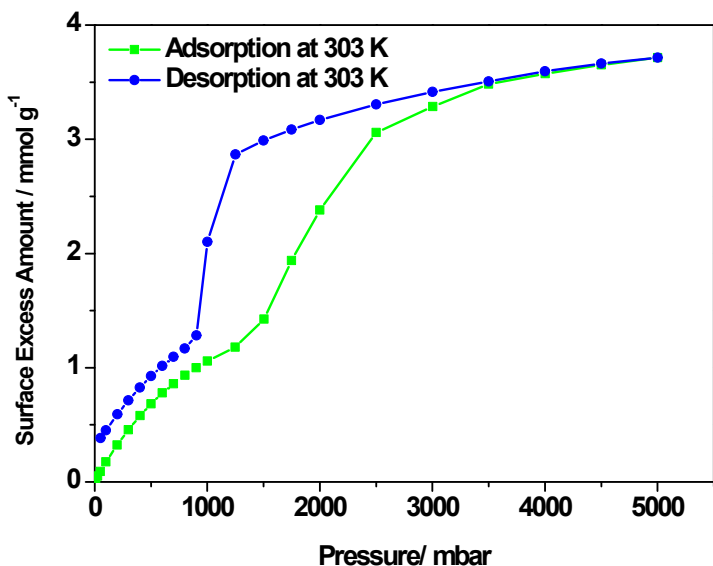
c)



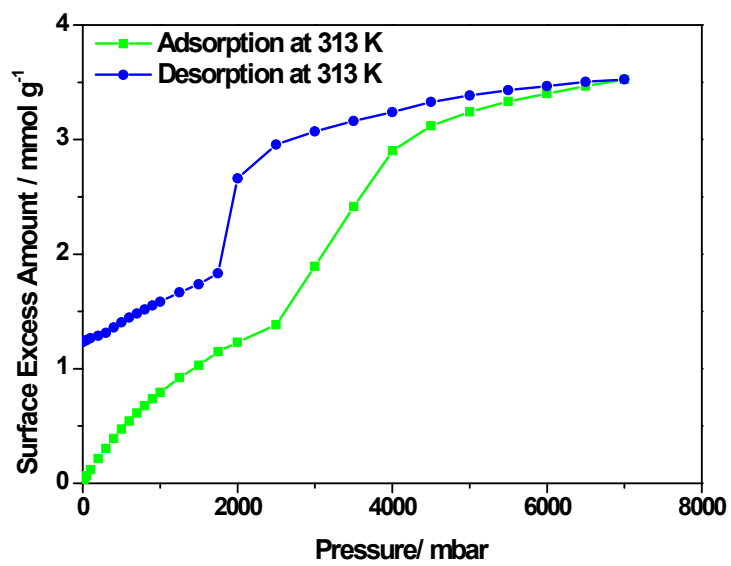
d)



e)



f)



g)

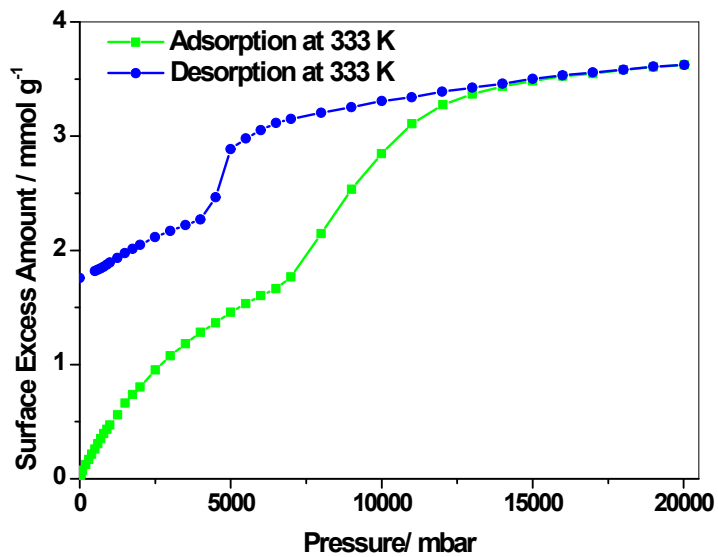


Figure S3. High pressure CO adsorption/desorption isotherms for $\text{NaNi}_3(\text{OH})(\text{SIP})_2$ a) low pressure comparison b) 273 K, c) 283 K, d) 293 K, e) 303 K, f) 313 K and g) 333 K

S2.1.2 CO low pressure desorption kinetic profiles at 348 K

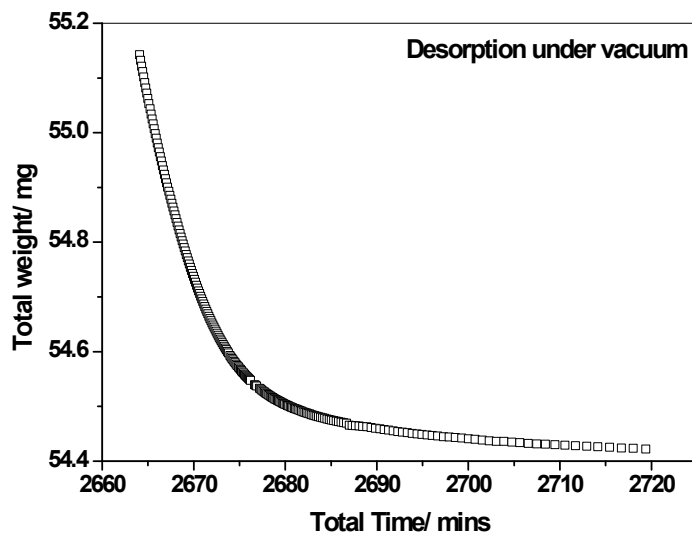
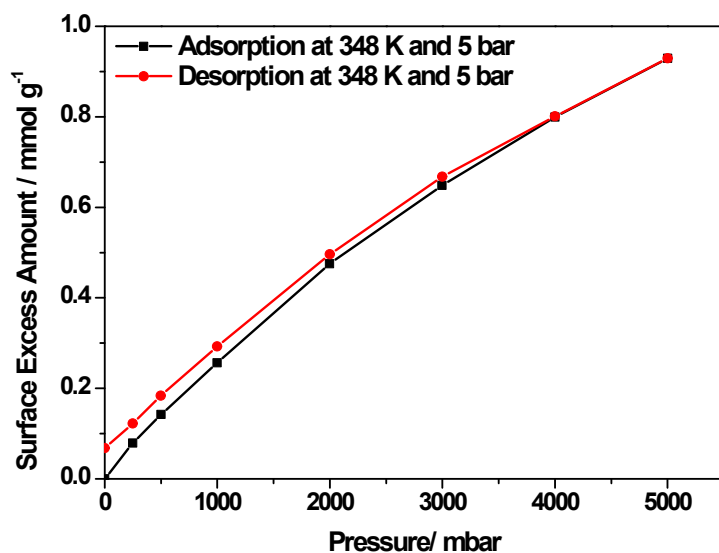


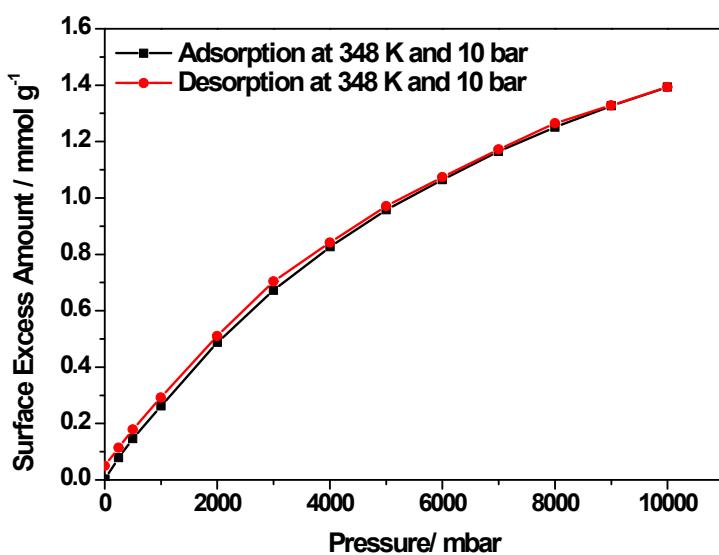
Figure S4: Carbon monoxide desorption kinetic profile for $\text{NaNi}_3(\text{OH})(\text{SIP})_2$ under ultra-high vacuum at 348 K

S2.1.3 CO loading experiments

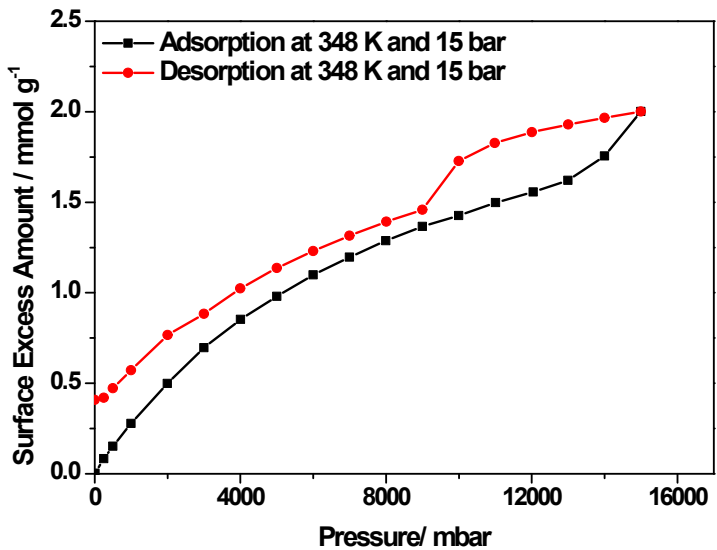
a)



b)



c)



d)

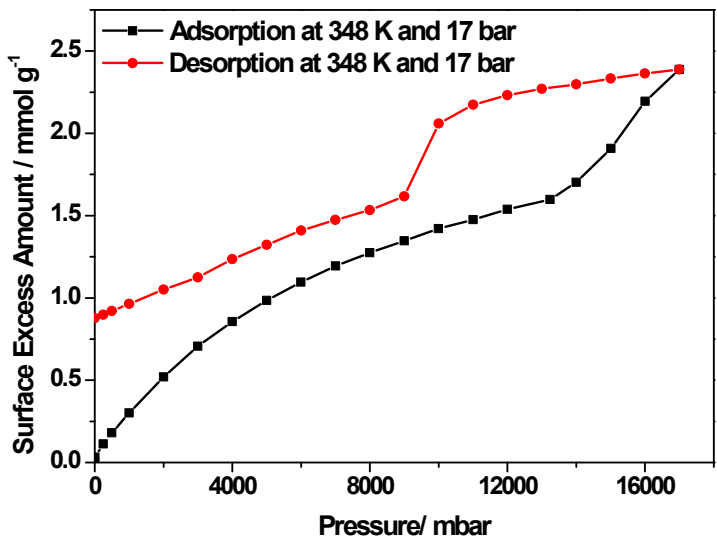


Figure S5. CO adsorption/ desorption isotherms for $\text{NaNi}_3(\text{OH})(\text{SIP})_2$ at 348 K for maximum pressures of a) 5 bar, b) 10 bar, c) 15 bar, d) 17 bar.

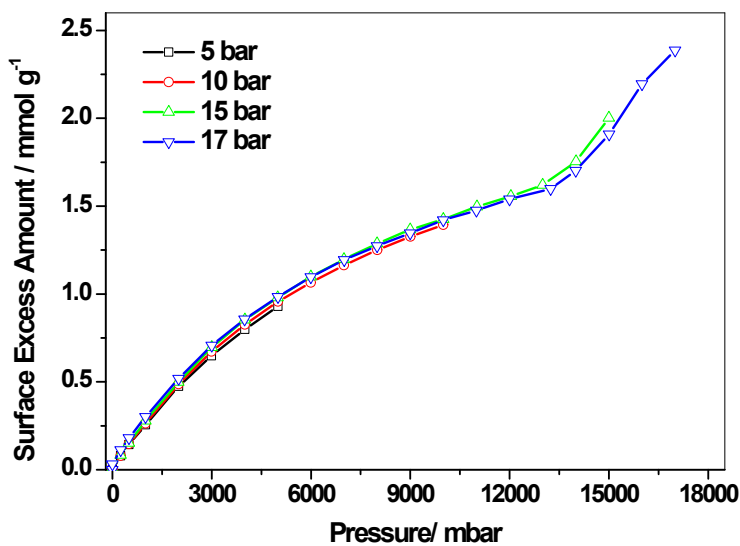


Figure S6. Repeatability of CO adsorption isotherm loading experiments for different samples of $\text{NaNi}_3(\text{OH})(\text{SIP})_2$ at 348 K over the pressure range 5 – 17 bar.

S2.1.4 Activation of $\text{NaNi}_3(\text{OH})(\text{SIP})_2(\text{H}_2\text{O})_5 \cdot \text{H}_2\text{O}$ under ultra-high vacuum at 403 K to give $\text{NaNi}_3(\text{OH})(\text{SIP})_2(\text{H}_2\text{O})_2$ for comparison with XRD measurements

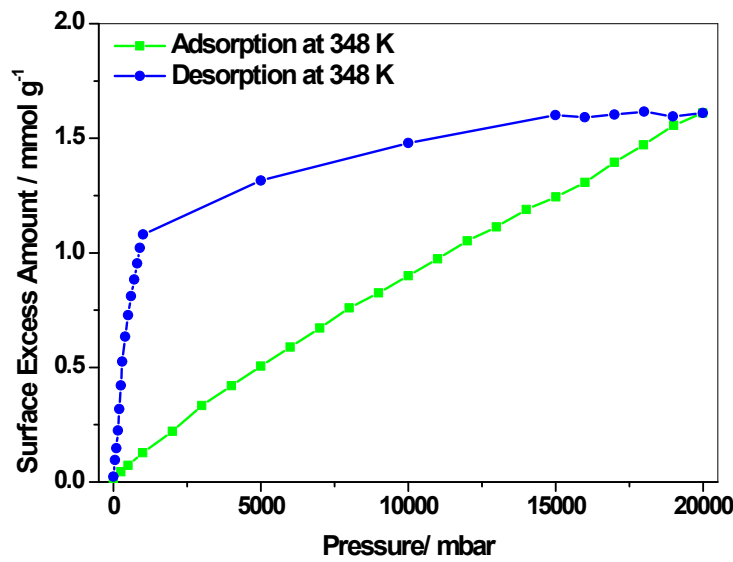


Figure S7. CO adsorption/ desorption isotherms at 348 K up to 20 bar for $\text{NaNi}_3(\text{OH})(\text{SIP})_2(\text{H}_2\text{O})_2$

S2.1.5 CO Desorption kinetics for $\text{NaNi}_3(\text{OH})(\text{SIP})_2(\text{H}_2\text{O})_2$ degassed at 403 K

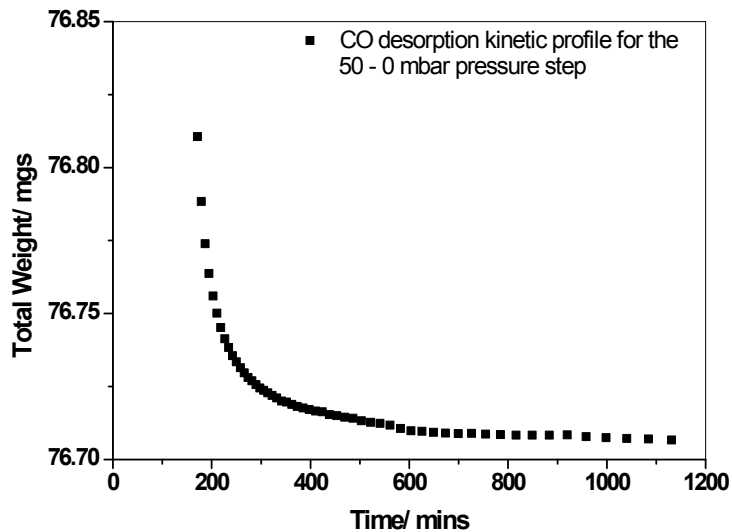
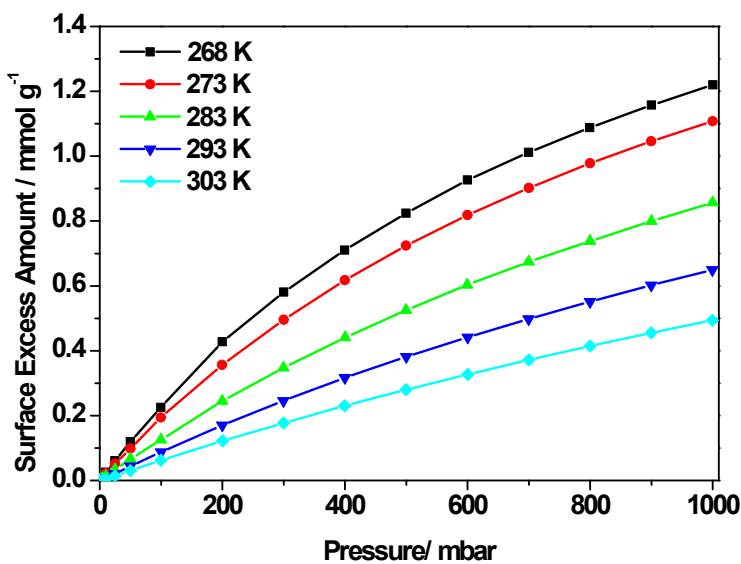


Figure S8. Kinetic profile for desorption of CO from $\text{NaNi}_3(\text{OH})(\text{SIP})_2(\text{H}_2\text{O})_2$ for pressure decrement 250 – 0 mbar

S2.2 $\text{NaCo}_3(\text{OH})(\text{SIP})_2$

S2.2.1 CO adsorption/desorption isotherms for $\text{NaCo}_3(\text{OH})(\text{SIP})_2$

a)



b)

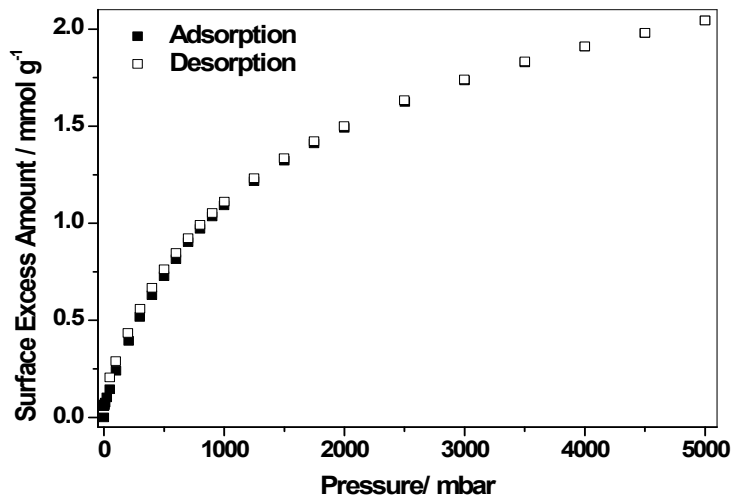


Figure S9. CO adsorption/ desorption isotherms on $\text{NaCo}_3(\text{OH})(\text{SIP})_2$ a) 268 – 303 K up to 1 bar and b) 348 K up to 5 bar

S2.2.2 CO desorption kinetics profile for $\text{NaCo}_3(\text{OH})(\text{SIP})_2$

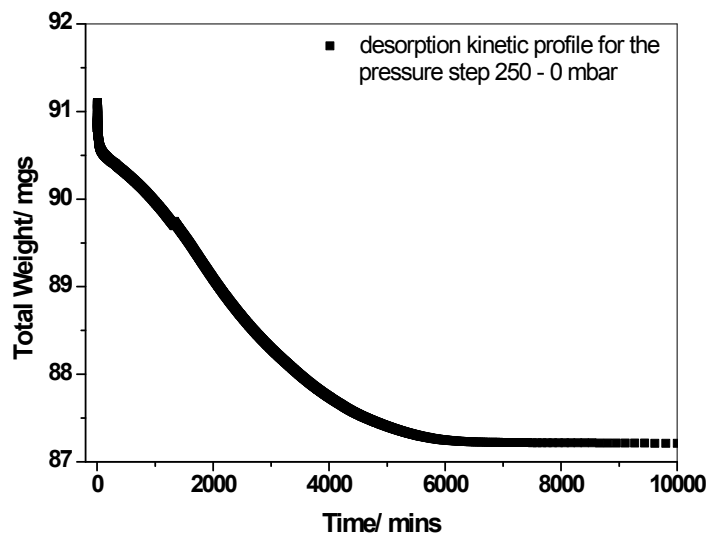
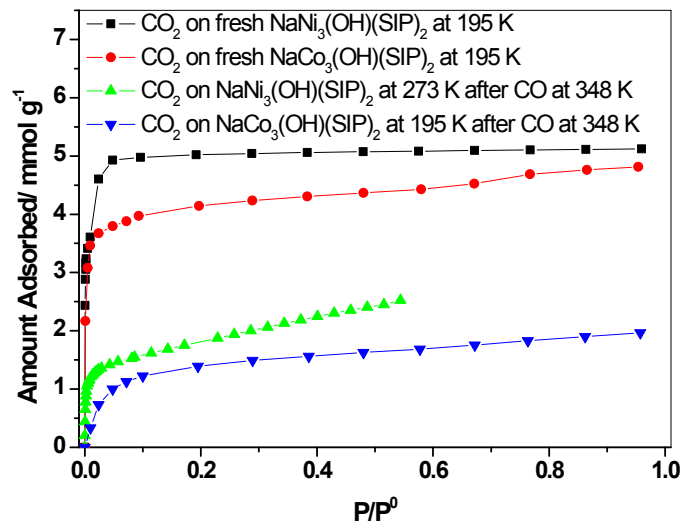


Figure S10. Kinetic profile for desorption of CO at 348 K from $\text{NaCo}_3(\text{OH})(\text{SIP})_2$ for pressure decrement 250 – 0 mbar

S3.0 Comparison of carbon dioxide adsorption isotherms before and after CO Adsorption



b)

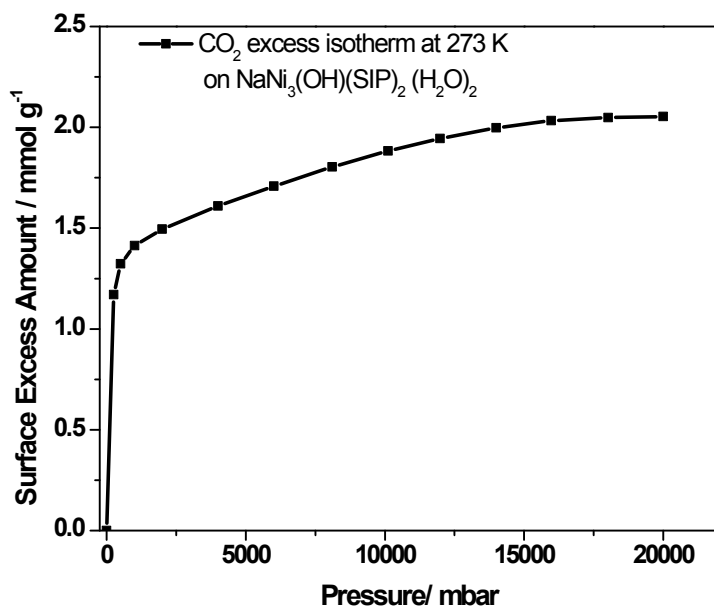


Figure S11. CO₂ adsorption isotherms basis a) Comparison on a relative pressure of NaNi₃(OH)(SIP)₂ and NaCo₃(OH)(SIP)₂ at 195 K prior to CO treatment with NaNi₃(OH)(SIP)₂ and NaCo₃(OH)(SIP)₂ after CO adsorption at 348 K b) NaNi₃(OH)(SIP)₂(H₂O)₂ at 273 K and up to 20 bar

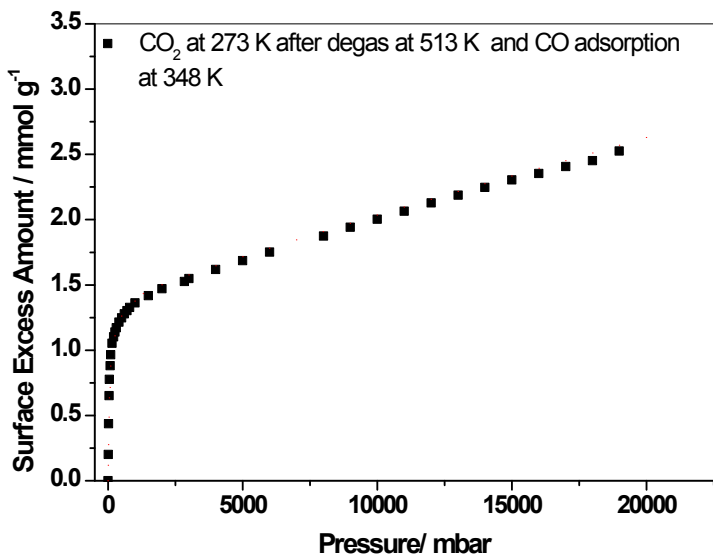


Figure S12. Isotherm for CO₂ Adsorption at 273 K for NaNi₃(OH)(SIP)₂ degassed at 513K after CO adsorption at 348 K

S4.0 Virial analysis

S4.1 CO adsorption on NaNi₃(OH)(SIP)₂ (Degas Temperature 513 K)

Table S1. Virial Parameters for CO Adsorption on NaNi₃(OH)(SIP)₂ (Degas Temperature 513 K) in the Temperature Range 273 – 343 K

| Temperature (K) | Temperature error (K) | A ₀ (ln(mol g ⁻¹ Pa ⁻¹)) | A ₀ error (ln(mol g ⁻¹ Pa ⁻¹)) | A ₁ (g mol ⁻¹) | A ₁ error (g mol ⁻¹) |
|-----------------|-----------------------|--|--|---------------------------------------|---|
| 273.125 | 0.004 | -16.105 | 0.015 | -347.5 | 20.6 |
| 283.140 | 0.008 | -16.645 | 0.036 | -498.8 | 56.8 |
| 293.139 | 0.009 | -17.090 | 0.020 | -605.5 | 28.5 |
| 303.125 | 0.004 | -17.613 | 0.011 | -598.7 | 14.6 |
| 313.137 | 0.007 | -18.120 | 0.005 | -517.7 | 7.7 |
| 323.134 | 0.013 | -18.539 | 0.004 | -539.5 | 7.7 |
| 333.105 | 0.005 | -18.856 | 0.005 | -712.7 | 13.3 |
| 343.114 | 0.007 | -19.212 | 0.004 | -676.8 | 15.9 |

Table S2. Virial Parameters for CO Adsorption on NaCo₃(OH)(SIP)₂ (Degas Temperature 448 K) in the Temperature Range 268 – 303 K

| Temperature (K) | Temperature error (K) | $A_0 (\ln(\text{mol g}^{-1} \text{Pa}^{-1}))$ | $A_0 \text{ error } (\ln(\text{mol g}^{-1} \text{Pa}^{-1}))$ | $A_1 (\text{g mol}^{-1})$ | $A_1 \text{ error } (\text{g mol}^{-1})$ |
|-----------------|-----------------------|---|--|---------------------------|--|
| 268.139 | 0.041 | -17.479 | 0.012 | -522.3 | 22.5 |
| 273.120 | 0.010 | -17.633 | 0.009 | -586.9 | 12.6 |
| 283.135 | 0.013 | -18.102 | 0.010 | -529.6 | 18.8 |
| 293.146 | 0.010 | -18.491 | 0.006 | -542.8 | 13.6 |
| 303.124 | 0.004 | -18.849 | 0.003 | -550.3 | 10.1 |

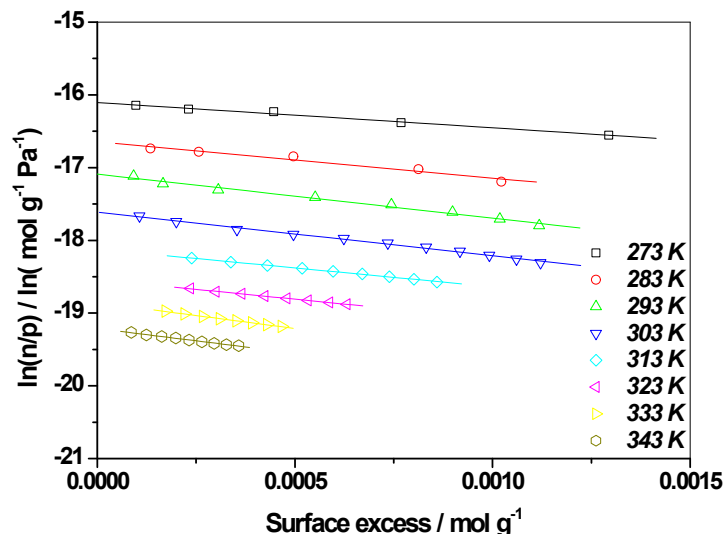


Figure S13. The variation of $\ln(n/p)$ vs. surface excess for CO adsorption on $\text{NaNi}_3(\text{OH})(\text{SIP})_2$ (degas temperature 513 K) over the temperature range 273 – 343 K and up to 1 bar

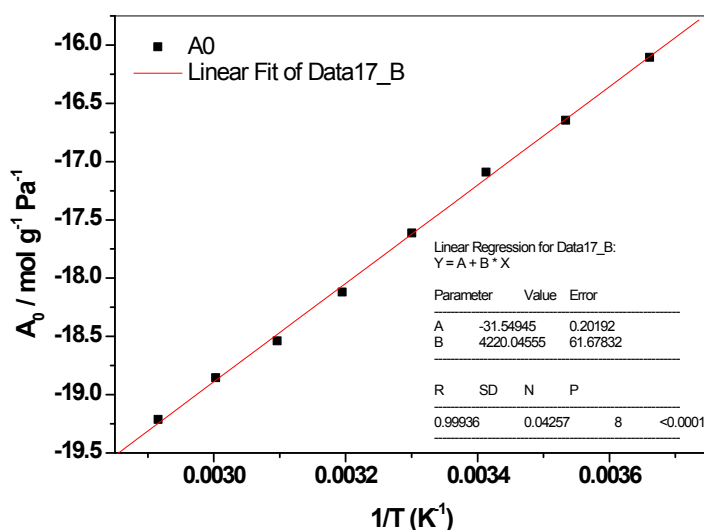


Figure S14. Graph of A_0 vs. $1/T$ for CO adsorption on $\text{NaNi}_3(\text{OH})(\text{SIP})_2$ (degas temperature 513 K) over the temperature range 273 – 343 K

S4.2 CO adsorption on NaCo₃(OH)(SIP)₂

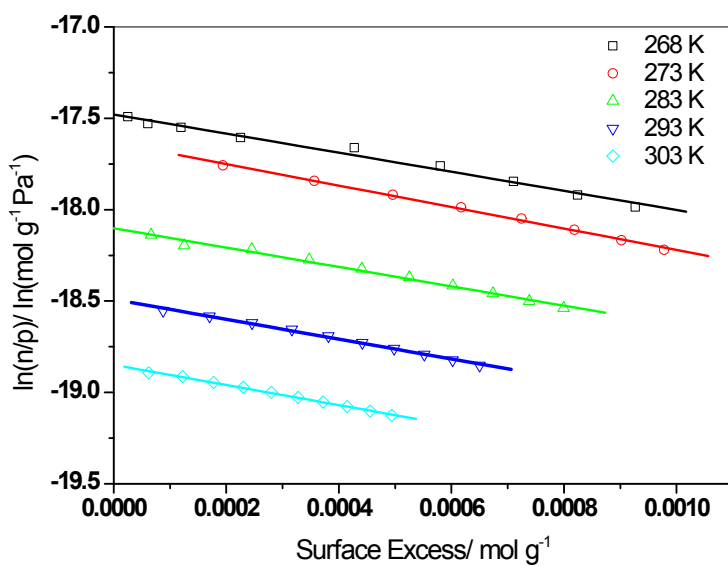


Figure S15. Graphs of $\ln(n/p)$ vs. surface excess for CO adsorption on $\text{NaCo}_3(\text{OH})(\text{SIP})_2$ (degas temperature 448 K) over the temperature range 268 K – 303 K

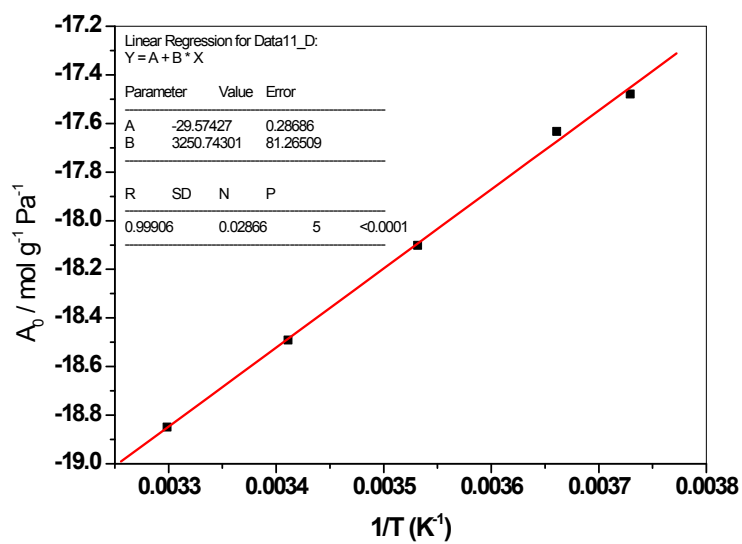


Figure S16. Graphs of A_0 vs. $1/T$ for CO adsorption on $\text{NaCo}_3(\text{OH})(\text{SIP})_2$ (degas temperature 448 K) over the temperature range 268 K – 303 K

S5.0 Clausius-Clapeyron graphs

S5.1 CO adsorption on $\text{NaNi}_3(\text{OH})(\text{SIP})_2$

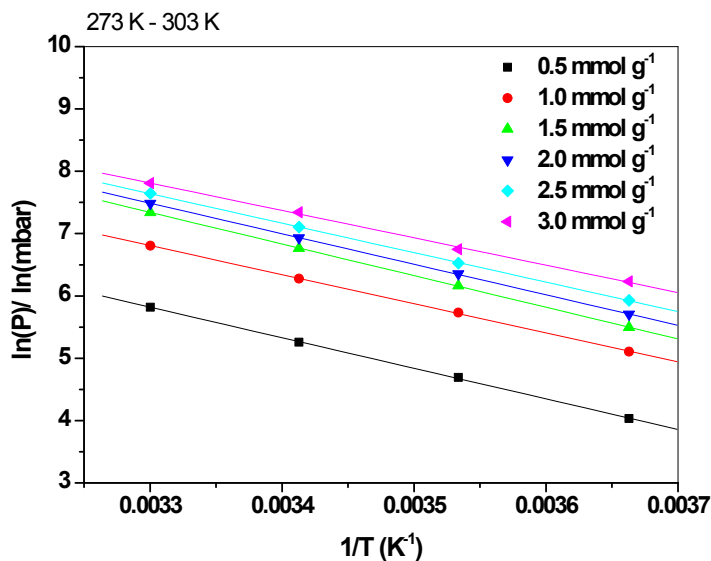


Figure S17. Graphs of $\ln(P)$ vs. $1/T$ for CO adsorption on $\text{NaNi}_3(\text{OH})(\text{SIP})_2$ over the temperature range 273 K - 303 K and uptake range 0.5 - 3.0 mmol g⁻¹

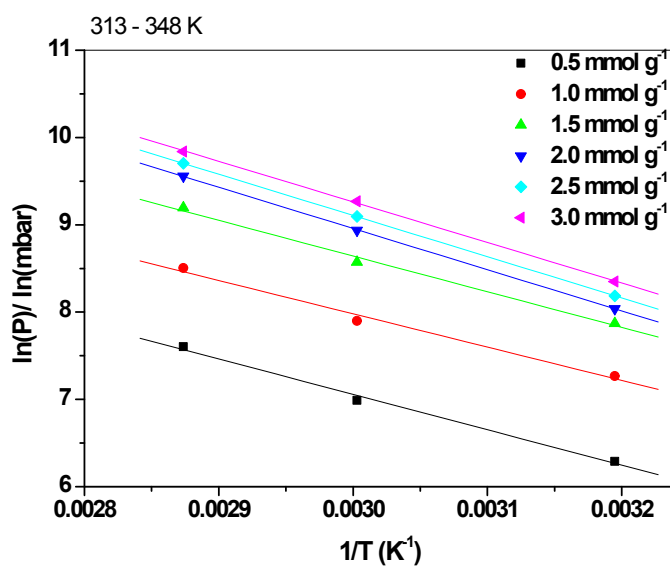


Figure S18. Graphs of $\ln(P)$ vs. $1/T$ for CO adsorption on $\text{NaNi}_3(\text{OH})(\text{SIP})_2$ over the temperature range 313 K – 348 K and uptake range 0.5 – 3.0 mmol g⁻¹

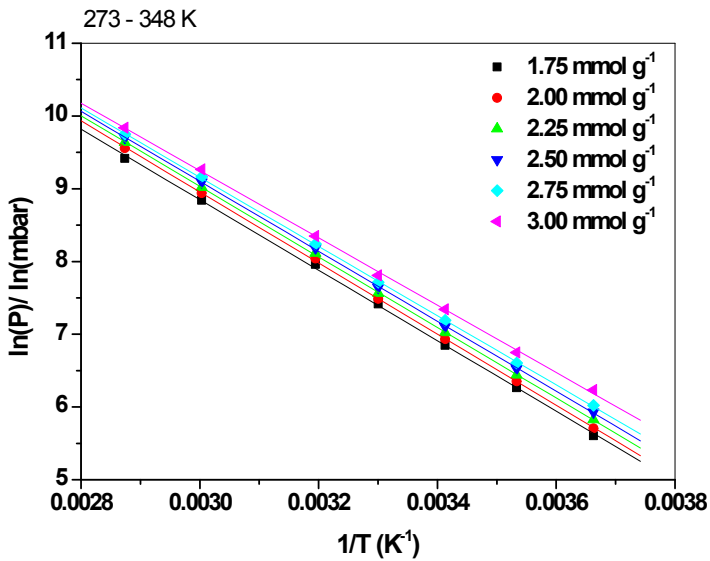
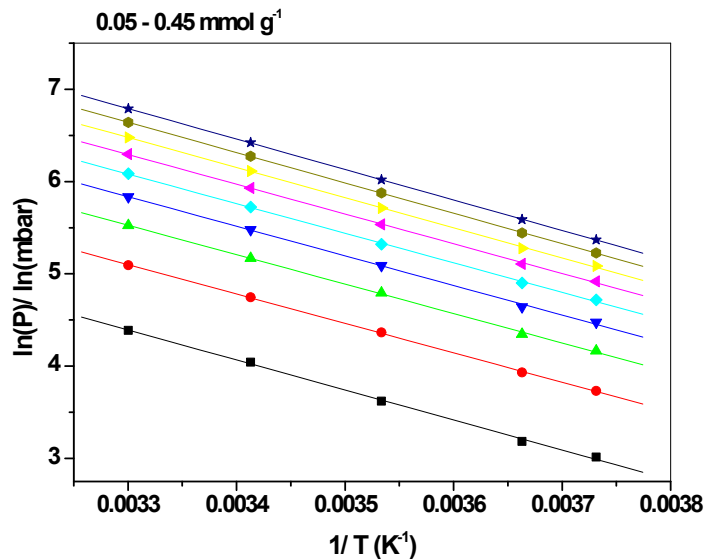


Figure S19. Graphs of $\ln(P)/\ln(\text{mbar})$ vs. $1/T$ for CO adsorption on $\text{NaNi}_3(\text{OH})(\text{SIP})_2$ over the temperature range 273 K – 348 K and uptake range after the point of isotherm inflection, which corresponds to $1.75 - 3.00 \text{ mmol g}^{-1}$.

S5.2 CO adsorption on $\text{NaCo}_3(\text{OH})_2(\text{SIP})_2$ (degas temperature 448 K)

a)



b)

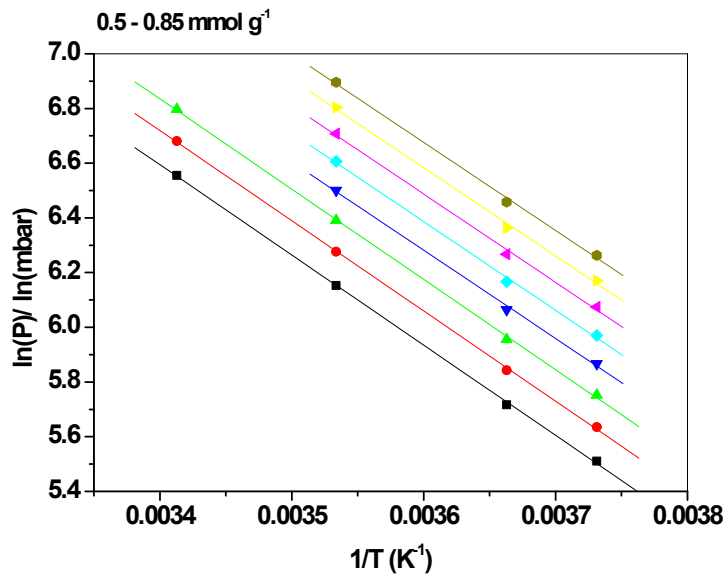


Figure S20. Graphs of $\ln(P)$ vs. $1/T$ for a) $0.05 - 0.45 \text{ mol g}^{-1}$ and b) $0.5 - 0.85 \text{ mol g}^{-1}$

S6.0 Enthalpy and entropy of adsorption for $\text{NaNi}_3(\text{OH})_2(\text{SIP})_2$ and $\text{NaCo}_3(\text{OH})(\text{SIP})_2$

Table S3. Enthalpy and Entropy of CO Adsorption on $\text{NaNi}_3(\text{OH})(\text{SIP})_2$: 273 – 303 K

| Amount Adsorbed/ mmol g^{-1} | Enthalpy of Adsorption/ kJ mol^{-1} | Error/ kJ mol^{-1} | Entropy of Adsorption/ kJ mol^{-1} | Error/ kJ mol^{-1} |
|--|--|-----------------------------|---|-----------------------------|
| 0.15 | 49.29 | 5.84 | -199.93 | 1.36 |
| 0.20 | 44.76 | 3.78 | -187.49 | 0.88 |
| 0.25 | 42.85 | 2.77 | -183.19 | 0.64 |
| 0.30 | 41.73 | 2.13 | -181.14 | 0.49 |
| 0.35 | 41.36 | 1.50 | -181.42 | 0.55 |
| 0.40 | 41.24 | 1.05 | -182.31 | 0.42 |
| 0.45 | 41.14 | 0.72 | -183.14 | 0.32 |
| 0.50 | 40.78 | 0.45 | -182.95 | 0.31 |
| 0.55 | 40.34 | 0.62 | -182.50 | 0.19 |
| 0.60 | 40.18 | 0.70 | -182.92 | 0.17 |
| 0.65 | 40.20 | 0.73 | -183.88 | 0.05 |
| 0.70 | 40.30 | 0.75 | -185.03 | 0.01 |
| 0.75 | 40.66 | 0.73 | -187.05 | 0.27 |
| 0.80 | 40.80 | 0.84 | -188.33 | 0.13 |
| 0.85 | 39.78 | 0.68 | -185.68 | 0.31 |
| 0.90 | 39.28 | 0.53 | -184.78 | 0.19 |
| 0.95 | 38.97 | 0.39 | -184.48 | 0.22 |
| 1.00 | 38.85 | 0.34 | -184.82 | 0.07 |

| | | | | |
|------|-------|------|---------|------|
| 1.05 | 38.81 | 0.59 | -185.45 | 0.33 |
| 1.10 | 39.12 | 0.72 | -187.26 | 0.16 |
| 1.15 | 40.16 | 0.87 | -191.49 | 0.28 |
| 1.20 | 41.26 | 0.65 | -195.69 | 0.56 |
| 1.25 | 41.80 | 0.89 | -197.91 | 0.65 |
| 1.30 | 42.06 | 0.71 | -199.05 | 0.24 |
| 1.35 | 42.26 | 0.43 | -199.94 | 0.36 |
| 1.40 | 42.44 | 0.20 | -200.79 | 0.34 |
| 1.45 | 42.42 | 0.15 | -200.91 | 0.17 |
| 1.50 | 42.22 | 0.18 | -200.37 | 0.05 |
| 1.55 | 42.03 | 0.22 | -199.86 | 0.05 |
| 1.60 | 41.84 | 0.25 | -199.37 | 0.05 |
| 1.65 | 41.67 | 0.27 | -198.93 | 0.02 |
| 1.70 | 41.52 | 0.27 | -198.53 | 0.01 |
| 1.75 | 41.37 | 0.28 | -198.16 | 0.01 |
| 1.80 | 41.22 | 0.28 | -197.79 | 0.01 |
| 1.85 | 41.08 | 0.28 | -197.45 | 0.01 |
| 1.90 | 40.94 | 0.28 | -197.11 | 0.01 |
| 1.95 | 40.83 | 0.28 | -196.86 | 0.01 |
| 2.00 | 40.73 | 0.23 | -196.69 | 0.07 |
| 2.05 | 40.56 | 0.14 | -196.25 | 0.11 |
| 2.10 | 40.40 | 0.06 | -195.83 | 0.11 |
| 2.15 | 40.23 | 0.02 | -195.42 | 0.08 |
| 2.20 | 40.07 | 0.04 | -194.99 | 0.04 |
| 2.25 | 39.91 | 0.07 | -194.58 | 0.04 |
| 2.30 | 39.75 | 0.10 | -194.19 | 0.04 |
| 2.35 | 39.60 | 0.12 | -193.81 | 0.04 |
| 2.40 | 39.49 | 0.16 | -193.57 | 0.05 |
| 2.45 | 39.43 | 0.20 | -193.52 | 0.08 |
| 2.50 | 39.38 | 0.25 | -193.48 | 0.08 |
| 2.55 | 39.32 | 0.30 | -193.44 | 0.08 |
| 2.60 | 39.29 | 0.29 | -193.47 | 0.05 |
| 2.65 | 39.27 | 0.26 | -193.59 | 0.18 |
| 2.70 | 38.93 | 0.40 | -192.60 | 0.22 |
| 2.75 | 38.54 | 0.58 | -191.43 | 0.26 |
| 2.80 | 38.16 | 0.74 | -190.32 | 0.25 |
| 2.85 | 37.81 | 0.89 | -189.27 | 0.24 |
| 2.90 | 37.47 | 1.04 | -188.28 | 0.24 |
| 2.95 | 37.06 | 0.93 | -187.06 | 0.16 |
| 3.00 | 36.54 | 1.05 | -185.53 | 0.43 |
| 3.05 | 35.85 | 1.61 | -183.47 | 1.05 |
| 3.10 | 35.63 | 1.93 | -183.10 | 0.54 |
| 3.15 | 35.41 | 2.02 | -182.76 | 0.35 |

Table S4. Enthalpy and entropy of CO adsorption on NaNi₃(OH)(SIP)₂: 313 – 348 K

| Amount Adsorbed/ mmol g⁻¹ | Enthalpy of Adsorption/ kJ mol⁻¹ | Error/ kJ mol⁻¹ | Entropy of Adsorption/ kJ mol⁻¹ | Error/ kJ mol⁻¹ |
|---|--|-----------------------------------|---|-----------------------------------|
| 0.10 | 34.42 | 5.73 | -146.16 | 5.74 |
| 0.15 | 33.82 | 3.67 | -148.40 | 2.34 |
| 0.20 | 33.95 | 3.18 | -151.60 | 0.69 |
| 0.25 | 33.78 | 2.68 | -153.26 | 0.70 |
| 0.30 | 33.78 | 2.99 | -155.00 | 0.48 |
| 0.35 | 33.85 | 3.38 | -156.69 | 0.59 |
| 0.40 | 33.88 | 3.48 | -158.08 | 0.16 |
| 0.45 | 33.91 | 2.99 | -159.34 | 0.81 |
| 0.50 | 33.71 | 2.57 | -159.81 | 0.68 |
| 0.55 | 33.72 | 2.48 | -160.84 | 0.14 |
| 0.60 | 33.55 | 2.89 | -161.23 | 0.73 |
| 0.65 | 33.30 | 3.36 | -161.24 | 0.87 |
| 0.70 | 33.02 | 3.17 | -161.22 | 0.29 |
| 0.75 | 32.77 | 2.87 | -161.27 | 0.52 |
| 0.80 | 32.50 | 2.40 | -161.21 | 0.83 |
| 0.85 | 32.06 | 2.39 | -160.54 | 0.04 |
| 0.90 | 31.96 | 2.60 | -160.90 | 0.42 |
| 0.95 | 31.88 | 3.04 | -161.34 | 0.89 |
| 1.00 | 31.71 | 3.13 | -161.47 | 0.21 |
| 1.05 | 31.75 | 3.24 | -162.22 | 0.22 |
| 1.10 | 31.94 | 3.13 | -163.38 | 0.25 |
| 1.15 | 32.18 | 2.92 | -164.66 | 0.49 |
| 1.20 | 31.75 | 3.11 | -163.99 | 0.48 |
| 1.25 | 31.35 | 3.26 | -163.36 | 0.40 |
| 1.30 | 31.19 | 3.45 | -163.48 | 0.45 |
| 1.35 | 31.08 | 3.36 | -163.74 | 0.18 |
| 1.40 | 31.41 | 3.27 | -165.20 | 0.27 |
| 1.45 | 32.57 | 2.98 | -169.10 | 0.90 |
| 1.50 | 33.98 | 2.61 | -173.78 | 1.08 |
| 1.55 | 35.07 | 2.00 | -177.46 | 1.45 |
| 1.60 | 36.02 | 1.30 | -180.71 | 1.53 |
| 1.65 | 36.70 | 0.33 | -183.10 | 1.99 |
| 1.70 | 37.28 | 0.12 | -185.13 | 0.89 |
| 1.75 | 37.75 | 0.39 | -186.79 | 0.52 |
| 1.80 | 38.13 | 0.33 | -188.16 | 0.12 |
| 1.85 | 38.48 | 0.13 | -189.39 | 0.39 |
| 1.90 | 38.80 | 0.05 | -190.53 | 0.35 |
| 1.95 | 39.11 | 0.22 | -191.64 | 0.32 |
| 2.00 | 39.25 | 0.27 | -192.23 | 0.09 |
| 2.05 | 39.31 | 0.26 | -192.53 | 0.03 |
| 2.10 | 39.36 | 0.24 | -192.83 | 0.03 |
| 2.15 | 39.41 | 0.23 | -193.12 | 0.02 |
| 2.20 | 39.43 | 0.20 | -193.29 | 0.06 |
| 2.25 | 39.42 | 0.15 | -193.39 | 0.09 |

| | | | | |
|------|-------|------|---------|------|
| 2.30 | 39.41 | 0.11 | -193.49 | 0.09 |
| 2.35 | 39.40 | 0.06 | -193.59 | 0.08 |
| 2.40 | 39.40 | 0.02 | -193.69 | 0.08 |
| 2.45 | 39.34 | 0.04 | -193.63 | 0.11 |
| 2.50 | 39.27 | 0.10 | -193.54 | 0.11 |
| 2.55 | 39.21 | 0.18 | -193.47 | 0.17 |
| 2.60 | 39.16 | 0.33 | -193.43 | 0.29 |
| 2.65 | 39.11 | 0.48 | -193.39 | 0.28 |
| 2.70 | 39.11 | 0.59 | -193.51 | 0.21 |
| 2.75 | 39.14 | 0.67 | -193.73 | 0.15 |
| 2.80 | 39.17 | 0.74 | -193.95 | 0.15 |
| 2.85 | 39.21 | 0.83 | -194.17 | 0.16 |
| 2.90 | 39.28 | 0.97 | -194.51 | 0.27 |
| 2.95 | 38.97 | 0.91 | -193.75 | 0.09 |
| 3.00 | 38.65 | 0.85 | -192.96 | 0.11 |
| 3.05 | 38.37 | 0.77 | -192.29 | 0.14 |
| 3.10 | 38.30 | 0.55 | -192.25 | 0.43 |
| 3.15 | 37.94 | 0.47 | -191.42 | 0.15 |

Table S5. Enthalpy and entropy of CO adsorption on NaNi₃(OH)(SIP)₂ (degas temperature 513 K): 273 – 348 K

| Amount Adsorbed/ mmol g⁻¹ | Enthalpy of Adsorption/ kJ mol⁻¹ | Error/ kJ mol⁻¹ | Entropy of Adsorption/ kJ mol⁻¹ | Error/ kJ mol⁻¹ |
|---|--|-----------------------------------|---|-----------------------------------|
| 0.00 | 35.06 | 0.52 | | |
| 1.70 | 40.10 | 0.49 | -193.63 | 1.62 |
| 1.75 | 40.28 | 0.43 | -194.43 | 2.53 |
| 1.80 | 40.40 | 0.38 | -194.97 | 2.99 |
| 1.85 | 40.48 | 0.33 | -195.40 | 2.14 |
| 1.90 | 40.55 | 0.29 | -195.80 | 1.69 |
| 1.95 | 40.62 | 0.25 | -196.18 | 1.45 |
| 2.00 | 40.62 | 0.23 | -196.32 | 1.33 |
| 2.05 | 40.57 | 0.21 | -196.29 | 1.33 |
| 2.10 | 40.52 | 0.19 | -196.27 | 1.36 |
| 2.15 | 40.46 | 0.18 | -196.24 | 1.32 |
| 2.20 | 40.39 | 0.18 | -196.16 | 1.28 |
| 2.25 | 40.32 | 0.18 | -196.06 | 1.27 |
| 2.30 | 40.25 | 0.18 | -195.97 | 1.38 |
| 2.35 | 40.18 | 0.18 | -195.88 | 1.54 |
| 2.40 | 40.11 | 0.18 | -195.79 | 1.61 |
| 2.45 | 40.04 | 0.18 | -195.68 | 1.70 |
| 2.50 | 39.97 | 0.18 | -195.58 | 1.76 |
| 2.55 | 39.90 | 0.18 | -195.50 | 1.70 |
| 2.60 | 39.83 | 0.18 | -195.40 | 1.72 |
| 2.65 | 39.74 | 0.17 | -195.24 | 1.77 |
| 2.70 | 39.56 | 0.20 | -194.82 | 1.90 |
| 2.75 | 39.38 | 0.24 | -194.39 | 2.09 |
| 2.80 | 39.20 | 0.29 | -193.98 | 2.32 |
| 2.85 | 39.04 | 0.34 | -193.60 | 2.66 |
| 2.90 | 38.91 | 0.40 | -193.33 | 2.92 |
| 2.95 | 38.75 | 0.42 | -192.99 | 3.00 |
| 3.00 | 38.47 | 0.47 | -192.32 | 2.95 |
| 3.05 | 38.05 | 0.59 | -191.22 | 2.93 |
| 3.10 | 37.68 | 0.62 | -190.30 | 2.83 |
| 3.15 | 37.30 | 0.62 | -189.41 | 2.55 |

Table S2. Enthalpy and entropy of CO adsorption on $\text{NaCo}_3(\text{OH})(\text{SIP})_2$ (degas temperature 448 K): 268 – 303 K

| Amount Adsorbed/ mmol g⁻¹ | Enthalpy of Adsorption/ kJ mol⁻¹ | Error/ kJ mol⁻¹ | Entropy of Adsorption/ kJ mol⁻¹ | Error/ kJ mol⁻¹ |
|---|--|-----------------------------------|---|-----------------------------------|
| 0 | 27.03 | 0.68 | | |
| 0.05 | 27.09 | 0.58 | -125.83 | 2.06 |
| 0.1 | 26.55 | 0.25 | -129.93 | 0.87 |
| 0.15 | 26.58 | 0.42 | -133.58 | 1.48 |
| 0.2 | 26.73 | 0.52 | -136.66 | 1.85 |
| 0.25 | 26.69 | 0.39 | -138.54 | 1.37 |
| 0.3 | 26.86 | 0.31 | -140.87 | 1.11 |
| 0.35 | 27.18 | 0.30 | -143.48 | 1.05 |
| 0.4 | 27.41 | 0.10 | -145.60 | 0.35 |
| 0.45 | 27.51 | 0.08 | -147.14 | 0.30 |
| 0.5 | 27.48 | 0.35 | -148.16 | 1.25 |
| 0.55 | 27.48 | 0.32 | -149.22 | 1.15 |
| 0.6 | 27.50 | 0.42 | -150.23 | 1.49 |
| 0.65 | 26.90 | 1.03 | -148.96 | 3.75 |
| 0.7 | 27.02 | 1.09 | -150.25 | 3.98 |
| 0.75 | 26.93 | 1.24 | -150.79 | 4.50 |
| 0.8 | 26.87 | 1.20 | -151.35 | 4.37 |
| 0.85 | 26.86 | 1.12 | -152.11 | 4.09 |

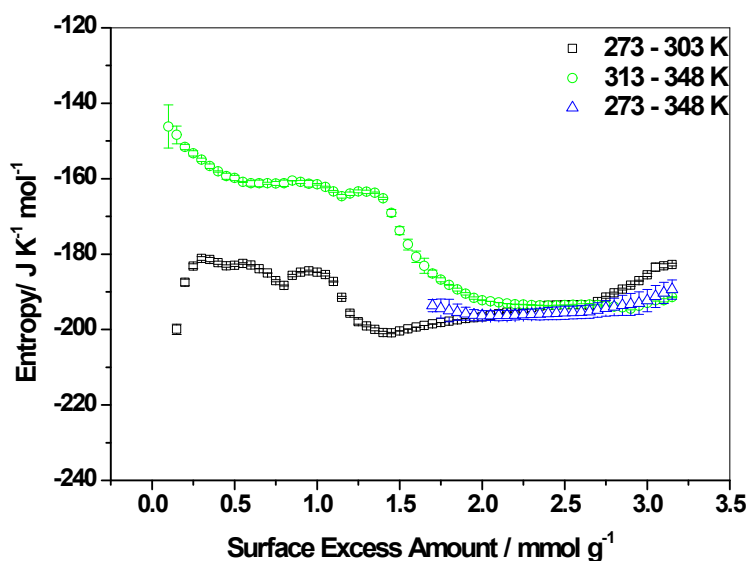


Figure S21. Graphs of entropy of adsorption vs. surface excess for CO adsorption on $\text{NaNi}_3(\text{OH})(\text{SIP})_2$ over the temperature range 273 – 348 K (excluding 323 K isotherm)

S7.0 Ideal adsorbed solution theory: CO/N₂ Selectivity

The adsorption of a CO/N₂ 50:50 mixture on NaNi₃(OH)(SIP)₂ and NaCo₃(OH)(SIP)₂ was modelled using ideal adsorbed solution theory.¹ The model requires no equilibrium mixture data, only pure component isotherms at equal temperature. The model is based on solving the following set of equations:

$$(1) \text{Py}_1 = P^0_1 x_1$$

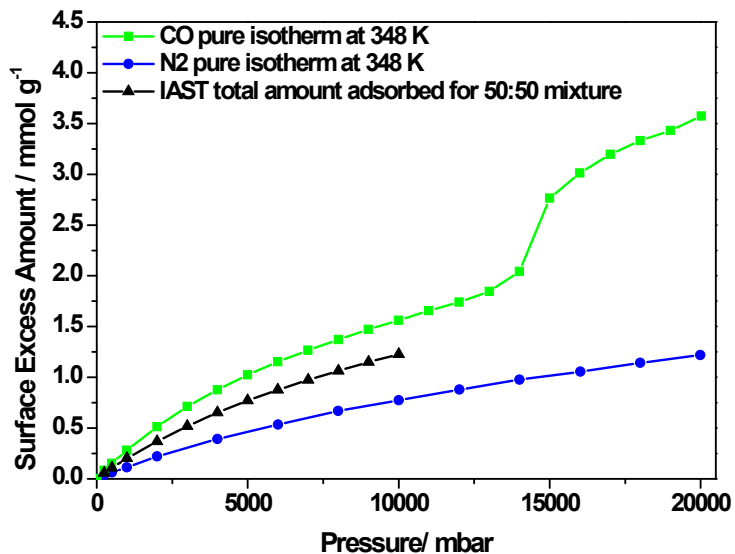
$$(2) P(1-y_1) = P^0_2(1-x_1)$$

$$(3) \int_{P=0}^{P=P_1^0} \frac{n_1^*(P)}{P} dP = \int_{P=0}^{P=P_2^0} \frac{n_2^*(P)}{P} dP$$

$$(4) \frac{1}{n} = \frac{x_1}{n_1^*(P_1^0)} + \frac{x_2}{n_2^*(P_2^0)}$$

Where P is the total pressure, P⁰_i is the pressure of component i, y_i is the mole fraction of the gas phase for component i, x_i is the adsorbed phase mole fraction of component i. Integration of pure component isotherms (n^{*}_i /P⁰_i vs. P⁰_i) (equation 3) was performed numerically using the trapezoid method.

S7.1 Comparison of CO and N₂ adsorption isotherms for NaNi₃(OH)(SIP)₂ and NaCo₃(OH)(SIP)₂ at 348 K



b)

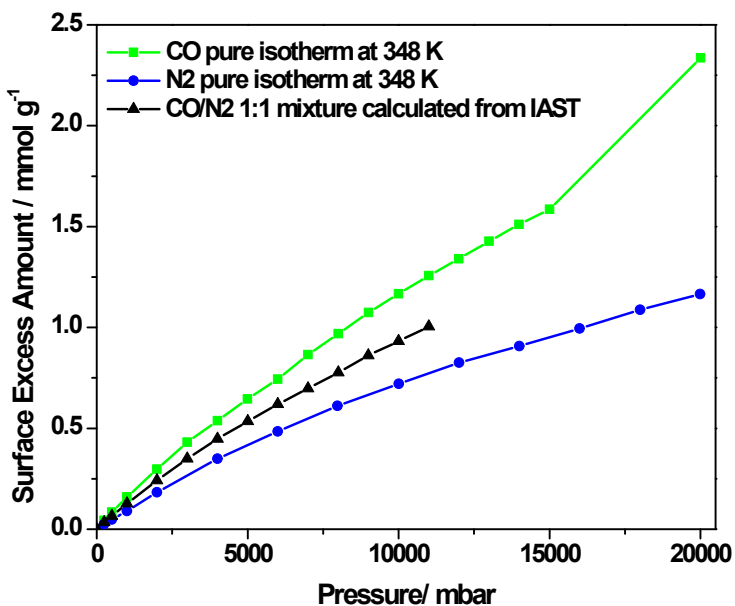
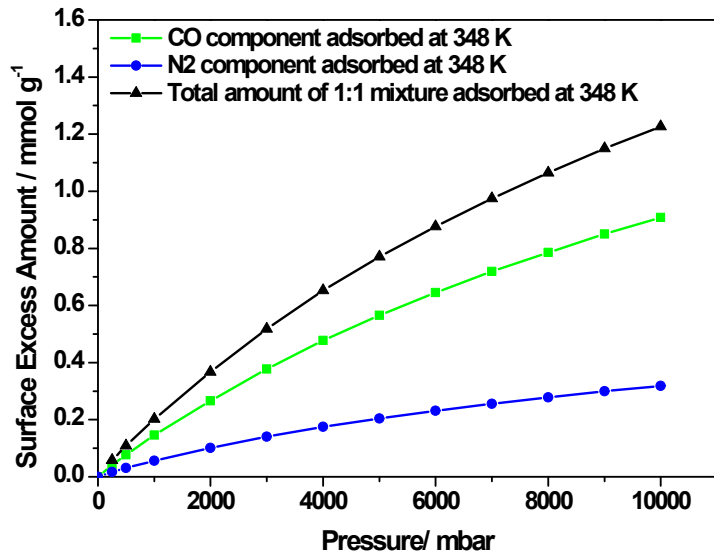


Figure S22. Surface excess adsorption isotherms for CO and N₂ and IAST calculations for 1:1 mixture at 348K on a) NaNi₃(OH)(SIP)₂ and b) NaCo₃(OH)(SIP)₂ at 348 K

a)



b)

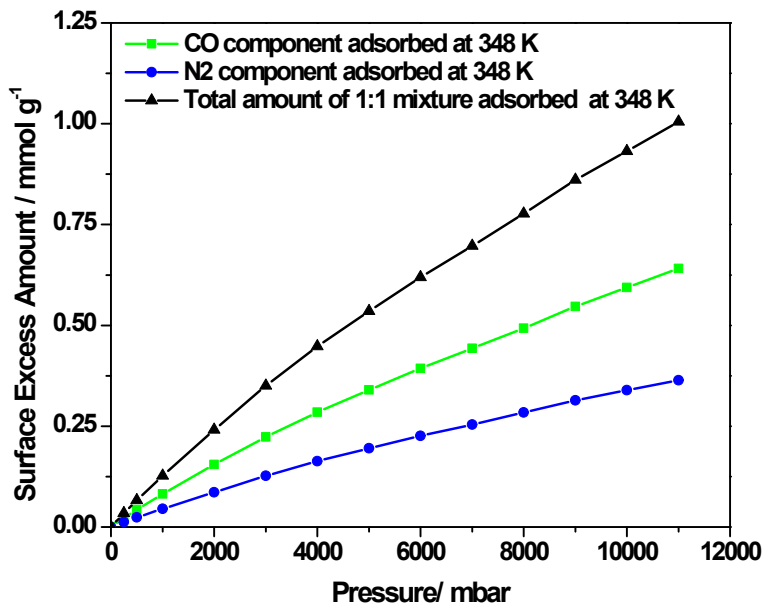
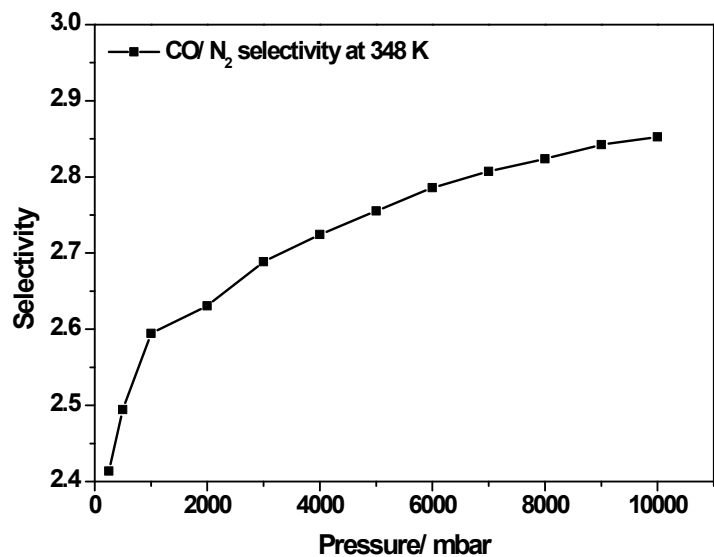


Figure S23. Comparison of surface excess adsorption isotherms for 1:1 CO/N₂ and components from IAST calculations at 348K on a) NaNi₃(OH)(SIP)₂ and b) NaCo₃(OH)(SIP)₂

S7.2 Comparison of CO/N₂ selectivity for adsorption of 1:1 mixture on NaNi₃(OH)(SIP)₂ and NaCo₃(OH)(SIP)₂ at 348 K

a)



b)

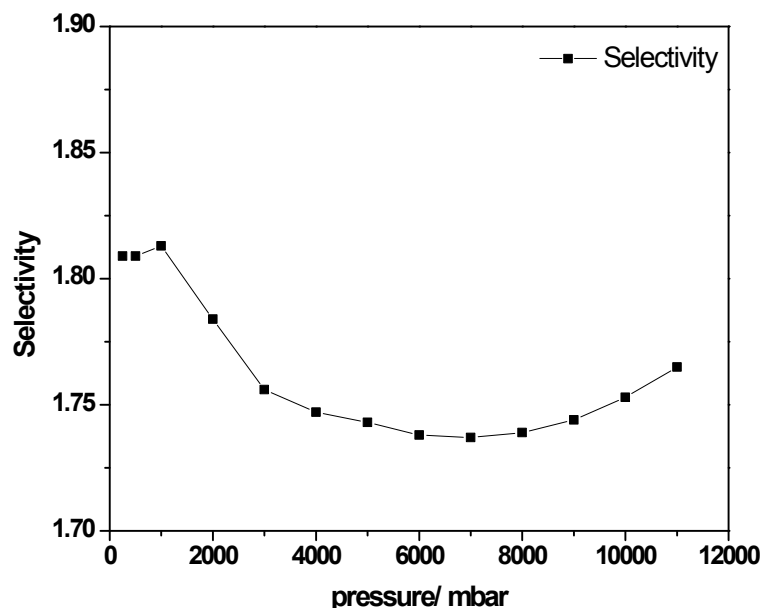


Figure S24. Selectivity for a 1:1 CO/N₂ mixture at 348 K calculated using ideal adsorbed solution theory for adsorption on a) NaNi₃(OH)(SIP)₂ and b) NaCo₃(OH)(SIP)₂

S8.0 In-situ temperature programmed desorption studies

S8.1 NaNi₃(OH)(SIP)₂

S8.1.1 In-situ Temperature Programmed Desorption under Ultra-High Vacuum after Sequential CO Isotherms

The sequential isotherm is Figure 6 in main text.

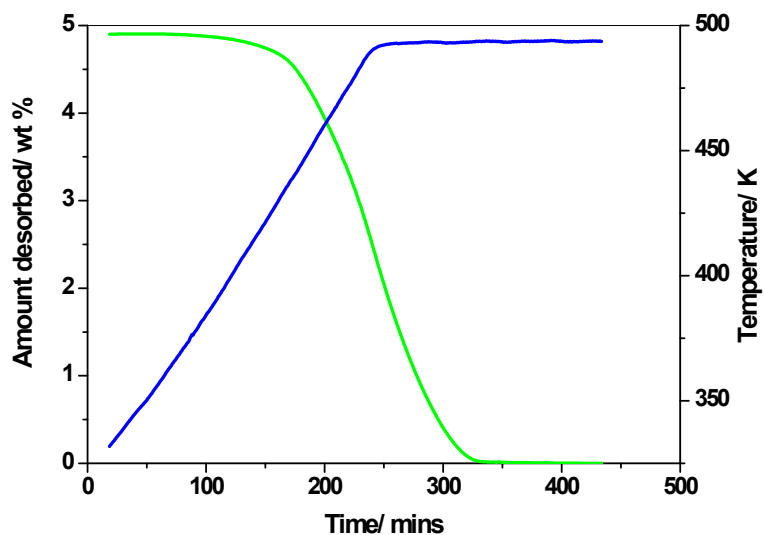
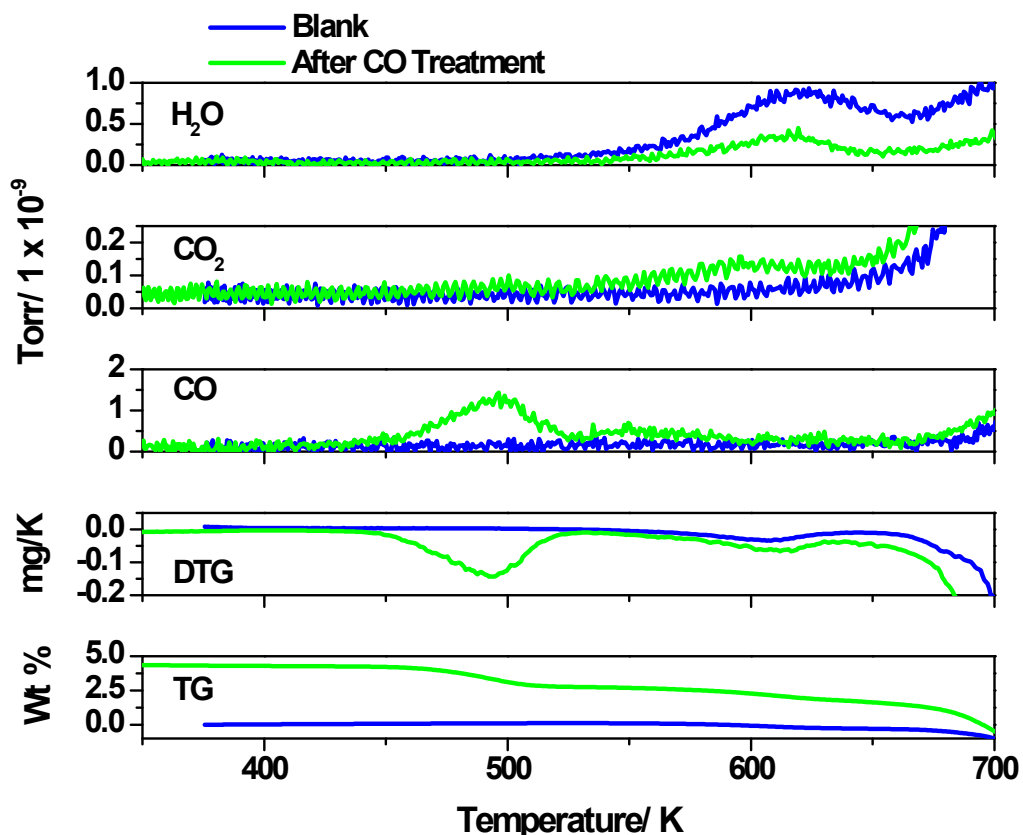


Figure S25. In-situ temperature programmed desorption in UHV after CO sequential isotherm for NaNi₃(OH)(SIP)₂ at 348 K: Amount of CO desorbed and temperature vs. time under UHV at a heating rate of 1K min⁻¹ to a maximum temperature of 493 K.

S8.1.2 In-situ temperature programmed desorption with simultaneous thermogravimetric and dynamic mass spectrometry under helium after CO treatment at 348 K

a)



b)

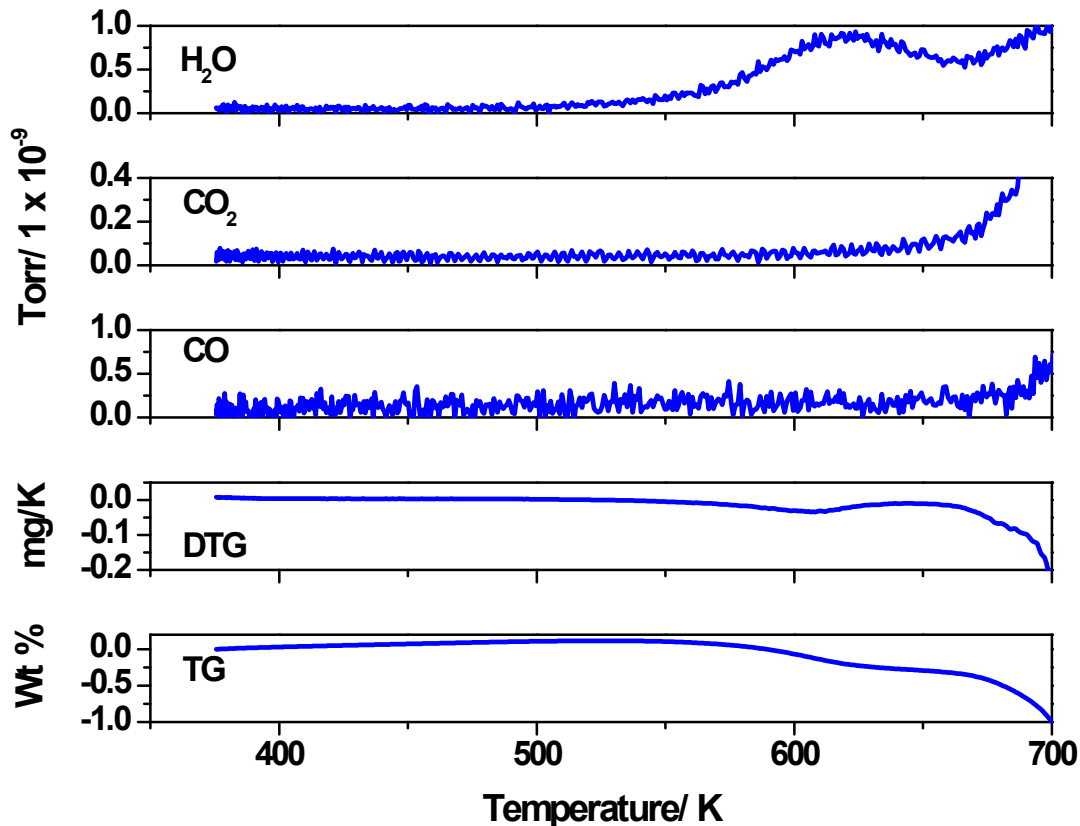


Figure S26: a) Comparison of temperature programmed thermogravimetric, differential thermogravimetric and gas evolution profiles from dynamic sampling mass spectrometry (DSMS) for $\text{NaNi}_3(\text{OH})(\text{SIP})_2$ (activation temperature 513 K) and $\text{NaNi}_3(\text{OH})(\text{SIP})_2$ after CO treatment at 348 K under dry helium (flow rate $50 \text{ cm}^3 \text{ min}^{-1}$) for CO, H_2O and CO_2 b) Temperature programmed thermogravimetric, differential thermogravimetric and gas evolution profiles from dynamic sampling mass spectrometry (DSMS) for $\text{NaNi}_3(\text{OH})(\text{SIP})_2$ (activation temperature 513 K) under dry helium (flow rate $50 \text{ cm}^3 \text{ min}^{-1}$) for CO, H_2O and CO_2

S9 Temperature programmed thermogravimetric analysis coupled with mass spectrometry in flowing helium (ex-situ measurements)

S9.1 Experimental

Thermogravimetric analysis (Thermal Sciences STA 1500 thermogravimetric analyzer) and mass spectrometry (VG Quadrupoles 300 amu) was used to investigate the decomposition of the MOFs. The desorbed species were monitored as a function of temperature during pyrolysis at 10 K min^{-1} in a flow of helium (60mL min^{-1}). The sampling probe inlet, which comprised of a 1 mm diameter stainless steel tube lined with a deactivated fused silica capillary was located $\sim 1\text{ cm}$ above the sample. This allows the detection of both stable decomposition products and reactive intermediate species.² Mass/charge ratios of 4(He), 18(H₂O), 28(CO), 32(O₂), 44(CO₂) and 64(SO₂), weight loss and sample temperature were monitored simultaneously throughout the TPD experiments.

S9.2 Results and discussion

Temperature programmed desorption profiles for fresh NaNi₃(OH)(SIP)₂ for CO, CO₂, SO₂ and H₂O were determined using TG-MS and are compared in Figure S27a. The TPD profiles for H₂O for NaNi₃(OH)(SIP)₂ show peaks at 478 K and 632 K before major framework decomposition. The higher noise level for the H₂O TPD profiles compared with the other profiles is due to the higher background H₂O signal present in the mass spectrometer. The lowest temperature peaks at 478 K corresponds to desorption of water adsorbed in the pores, whereas the peak at 632 K is due to decomposition of framework. Decomposition of the framework results in the production of CO, CO₂ and SO₂, with only comparatively small amounts of H₂O. The main CO and CO₂ TPD peaks coincided and occurred at $\sim 717\text{ K}$ with a weaker peak at 795 K. The TPD profiles show that the framework decomposition starts at $\sim 620\text{K}$. The TPD characteristics of NaCo₃(OH)(SIP)₂ are very similar to that of NaNi₃(OH)(SIP)₂. Figures S28-S32 show very similar CO, CO₂ and SO₂ TPD peaks for fresh and CO reacted NaNi₃(OH)(SIP)₂.

Mass spectrometer TPD peaks under helium at heating rate 20 K⁻¹

Table S3. Temperature Programmed Desorption peaks for Fresh
 $\text{NaNi}_3(\text{OH})(\text{SIP})_2(\text{H}_2\text{O})_5 \cdot \text{H}_2\text{O}$

| m/z | Peak 1 (K) | Peak 2 (K) | Peak 3 (K) |
|-----------------------|------------|------------|------------|
| 44 - CO ₂ | 717 | 748 | 795 |
| 28 - CO | 717 | 746 | 796 |
| 64 - SO ₂ | 724 | 740(sh) | |
| 18 - H ₂ O | 478 | 632 | |

(s) = shoulder

Table S4. Temperature Programmed Desorption peaks for Fresh
 $\text{NaCo}_3(\text{OH})(\text{SIP})_2(\text{H}_2\text{O})_5 \cdot \text{H}_2\text{O}$

| m/z | Peak 1 (K) | Peak 2 (K) | Peak 3 (K) | Peak 4 (K) |
|-----------------------|------------|------------|------------|------------|
| 44 - CO ₂ | (s) 687 | 733 | (s) 762 | 775 |
| 28 - CO | 732 | 763 | | |
| 64 - SO ₂ | 743 | | | |
| 18 - H ₂ O | 425 | 510 | | |

(s) = shoulder

Table S5. Temperature Programmed Desorption peaks for $\text{NaNi}_3(\text{OH})(\text{SIP})_2$ after exposure to CO at 348 K and 20 bar for 2 week

| m/z | Peak 1 (K) | Peak 2 (K) | Peak 3 (K) |
|----------------------|------------|------------|------------|
| 44 - CO ₂ | 719 | 749 | 800 |
| 28 - CO | 720 | 749 | 800 |
| 64 - SO ₂ | 724 | 742(sh) | |

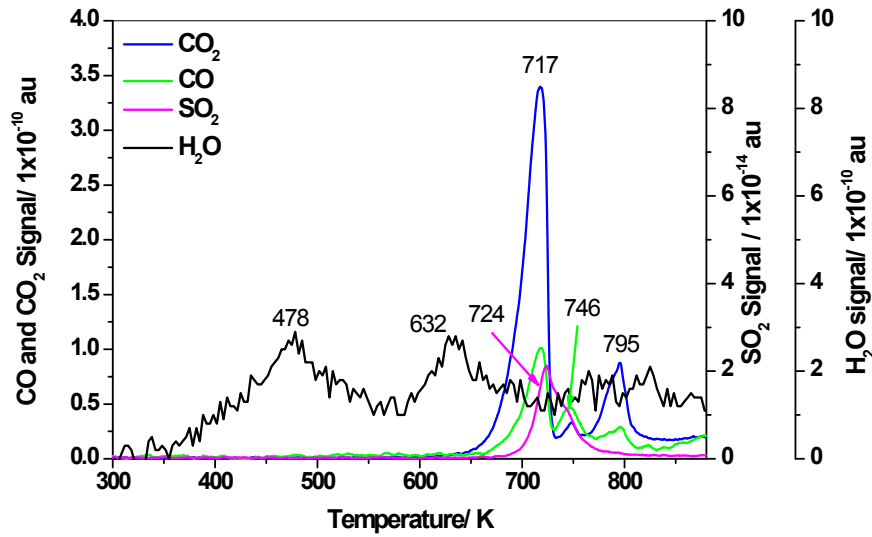
(s) = shoulder

Table S6. Temperature Programmed Desorption peaks for $\text{NaNi}_3(\text{OH})(\text{SIP})_2$ after exposure to CO at 373 K and 100 bar for 3 days

| m/z | Peak 1 (K) | Peak 2 (K) | Peak 3 (K) |
|----------------------|------------|------------|------------|
| 44 - CO ₂ | 716 | 745 | 797 |
| 28 - CO | 716 | 745 | 797 |
| 64 - SO ₂ | 724 | (s) 740 | |

(s) = shoulder

a)



b)

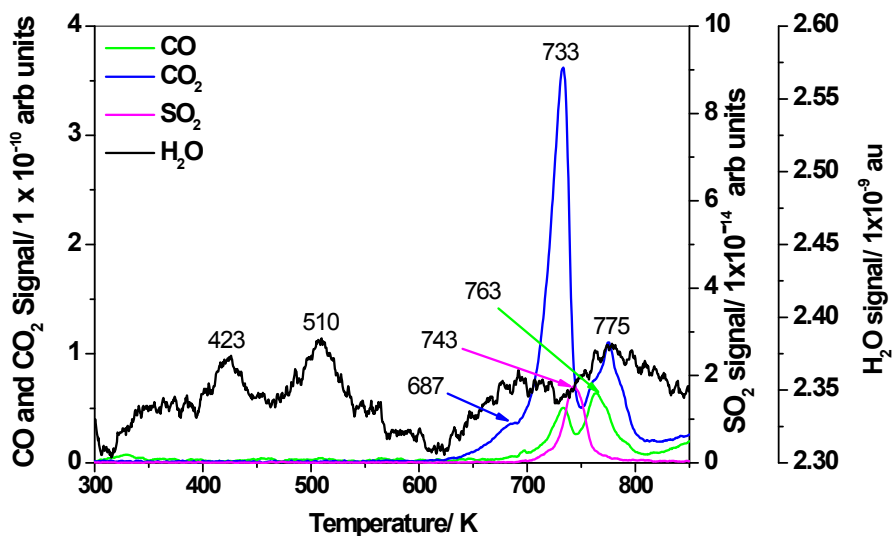


Figure S27. Temperature programmed desorption profiles of $m/z = 28(\text{CO})$, $44(\text{CO}_2)$ and $64(\text{SO}_2)$ peaks in flowing helium ($60 \text{ cm}^3 \text{ min}^{-1}$ for a) $\text{NaNi}_3(\text{OH})(\text{SIP})_2(\text{H}_2\text{O})_5 \cdot \text{H}_2\text{O}$ and b) $\text{NaCo}_3(\text{OH})(\text{SIP})_2(\text{H}_2\text{O})_5 \cdot \text{H}_2\text{O}$

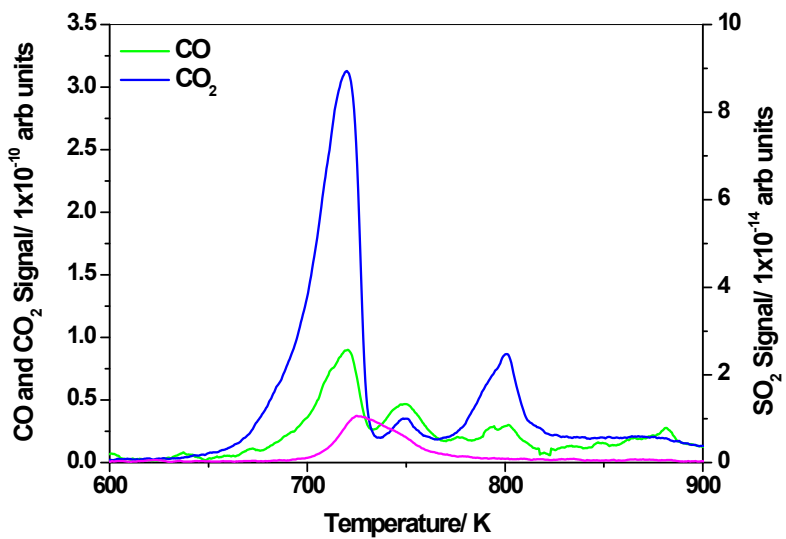


Figure S28. Temperature programmed desorption profiles of $m/z = 28(\text{CO})$, $44(\text{CO}_2)$ and $64(\text{SO}_2)$ for $\text{NaNi}_3(\text{OH})(\text{SIP})_2$ after exposure to CO at 348 K and up to 20 bar.

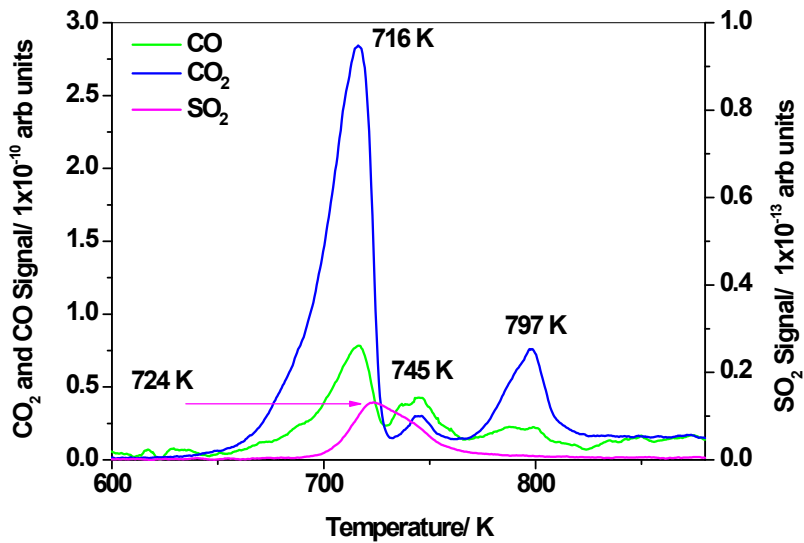


Figure S29 Temperature programmed desorption profiles of $m/z = 28(\text{CO})$, $44(\text{CO}_2)$ and $64(\text{SO}_2)$ for $\text{NaNi}_3(\text{OH})(\text{SIP})_2$ after exposure to CO at 373 K and at 100 bar in IMI-FLOW system.

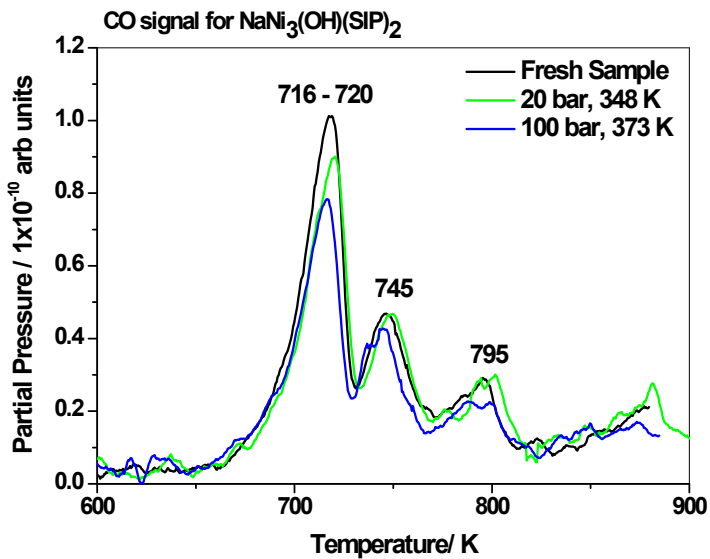


Figure S30. Temperature programmed desorption profiles of $m/z = 28(\text{CO})$ for fresh $\text{NaNi}_3(\text{OH})(\text{SIP})_2(\text{H}_2\text{O})_5 \cdot \text{H}_2\text{O}$, $\text{NaNi}_3(\text{OH})(\text{SIP})_2$ after CO isotherm at 348 K up to 20 bar and $\text{NaNi}_3(\text{OH})(\text{SIP})_2$ exposed to CO in IMI-FLOW at 373 K and 100 bar.

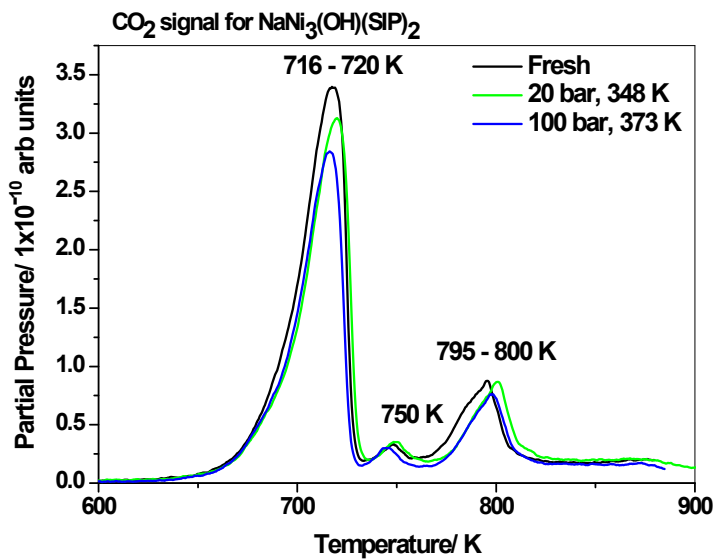


Figure S31. Temperature programmed desorption of $m/z = 44(\text{CO}_2)$ for fresh $\text{NaNi}_3(\text{OH})(\text{SIP})_2(\text{H}_2\text{O})_5 \cdot \text{H}_2\text{O}$, $\text{NaNi}_3(\text{OH})(\text{SIP})_2$ after CO isotherm at 348 K up to 20 bar and $\text{NaNi}_3(\text{OH})(\text{SIP})_2$ exposed to CO in IMI-FLOW at 373 K and 100 bar for three days.

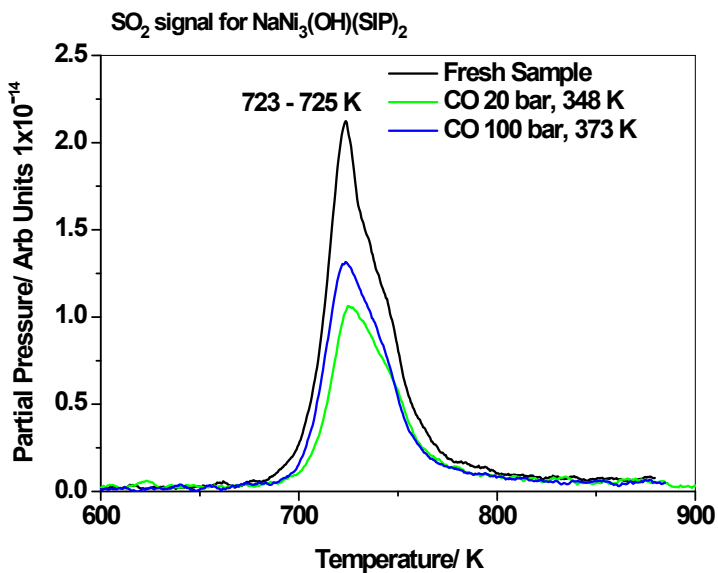


Figure S32. Temperature programmed desorption of $m/z = 64(\text{SO}_2)$ for fresh $\text{NaNi}_3(\text{OH})(\text{SIP})_2(\text{H}_2\text{O})_5 \cdot \text{H}_2\text{O}$, $\text{NaNi}_3(\text{OH})(\text{SIP})_2$ after CO isotherm at 348 K up to 20 bar and $\text{NaNi}_3(\text{OH})(\text{SIP})_2$ exposed to CO in IMI-FLOW at 373 K and 100 bar for three days

S10.0 Scanning electron microscopy

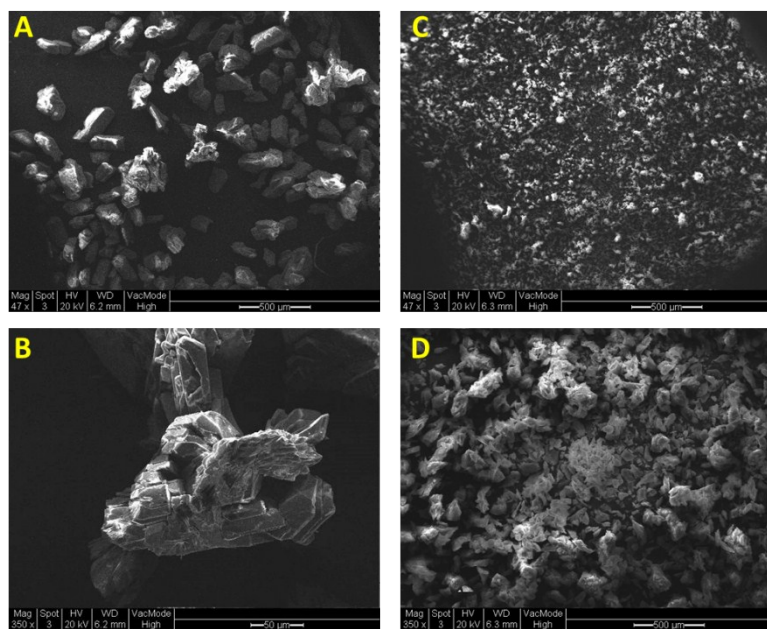


Figure S33. Scanning electron micrographs of fresh $\text{NaCo}_3(\text{OH})(\text{SIP})_2(\text{H}_2\text{O})_5 \cdot \text{H}_2\text{O}$ - A and B at x47 and x350, respectively and $\text{NaCo}_3(\text{OH})(\text{SIP})_2$ after CO adsorption at 348 K up to 20 bar - C and D at x47 and x350, respectively

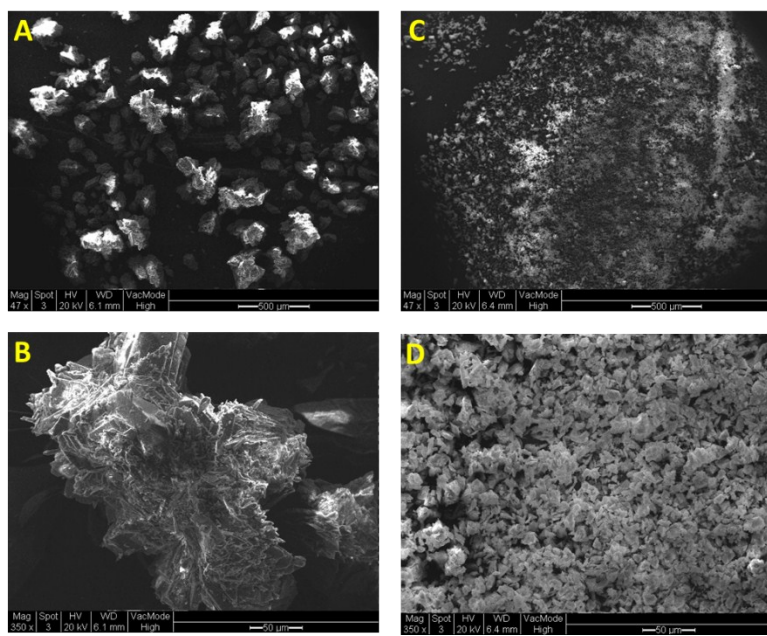


Figure S34. Scanning electron micrographs of fresh $\text{NaNi}_3(\text{OH})(\text{SIP})_2(\text{H}_2\text{O})_5 \cdot \text{H}_2\text{O}$ - A and B at x47 and x350, respectively and $\text{NaNi}_3(\text{OH})(\text{SIP})_2$ after CO adsorption at 348 K up to 20 bar - C and D at x47 and x350, respectively

References

1. Myers, A. L.; Prausnitz, J. M., Thermodynamics of mixed-gas adsorption. *Aiche Journal* **1965**, 11, (1), 121-127.
2. Jones, J. M.; Harding, A. W.; Brown, S. D.; Thomas, K. M., Detection of reactive intermediate nitrogen and sulphur species in the combustion of carbons that are models for coal chars. *Carbon* **1995**, 33, (6), 833-843.